DEPARTMENT OF GEOLOGY AND MINES

MINISTRY OF ECONOMIC AFFAIRS

Integrated Geo-Hazard Risk Assessment of Critical Landslides at Moshi, Samdrupjongkhar-Trashigang Highway, Wamrong Dungkhag under Trashigang Dzongkhag

Department of Geology and Mines

Field Season: 2014-2015

NAPA PROJECT

gef

UNDP

Empowered lives.
Resilient nations.

DEPARTMENT OF GEOLOGY AND MINES

MINISTRY OF ECONOMIC AFFAIRS

Integrated Geo-Hazard Risk Assessment of Critical Landslides at Moshi, Samdrupjongkhar-Trashigang Highway, Wamrong Dungkhag under Trashigang Dzongkhag

Department of Geology and Mines

Field Season: 2014-2015

ABOUT DEPARTMENT OF GEOLOGY & MINES (DGM)

Established in 1981 as Division initially and upgraded later to department, Department of Geology and Mines under Ministry of Economic Affairs is the only geo-scientific institution in the Kingdom of Bhutan mandated to carry out and manage geo-scientific and mining activities. Currently, the mandates of the department are fulfilled through four divisions namely: (1) Geological Survey Division; (2) Earthquake and Geophysics Division; (3) Mineral Development Division; and (4) Mining Division.

Contact Address: Department of Geology and Mines
Ministry of Economic Affairs
Royal Government of Bhutan
Thimphu: BHUTAN
P.O. Box: 173
Telephone: +975-2-323096
Web: www.moea.gov.bt

ABOUT THIS REPORT

This report is in accordance with the work plan of the Department of Geology and Mines, MoEA under the National Adaptation Programme of Action II (NAPA II) Project titled *'Addressing the Risks of Climate-Induced Disasters through Enhanced National and Local Capacity for Effective Actions*, funded by GEF-LDCF through UNDP and implemented by RGOB.

Report prepared by:
T.P. Thapa, Executive Geologist
Jamyang Chophel, Senior Engineering Geologist
Nedup Wangmo, Geologist
Jampel Gyeltshen, Senior Survey Engineer
Kinzang Duba, Survey Engineer

Reviewed by:

Ugyen Wangda, Chief Geologist

Tashi Tenzin, Project Manager, NAPA II Project, DGM

Suggested citation: Department of Geology and Mines (2018). *Integrated Geo-Hazard Risk Assessment of Critical Landslide at Moshi, Samdrupjongkhar-Trashigang Highway, Wamrong Dungkhag under Trashigang Dzongkhag.* Thimphu

Comments and inquiries on this report can be emailed at: jchophel@moea.gov.bt or tashit@moea.gov.bt

དཔལ་ལྡན་འབྲུག་གཞུང་ བསྒྲུབ་རྒྱས་ལྷན་ཁག།
སུ་ནི་དང་སྐ་གཏེར་ལས་ཁུངས་ ཐིམ་ཕུག།

Department of Geology and Mines
Ministry of Economic Affairs
Royal Government of Bhutan
Thimphu

Forward

Located in the eastern part of the Himalayas, the Kingdom of Bhutan is a small landlocked country between India and China. Being a part of young (ca. 55 million years) fold-thrust Himalayan mountain belt, more than 90 percent of the country's area is topographically rugged and geologically very fragile. In the foothills where rainfall is heavy during monsoon, the occurrence of landslides is significant. In recent years, landslide related risk to lives, livelihoods, infrastructures, properties and environment in the country is on rise because of intense and erratic rainfall pattern most likely induced by climate change and interactions of human activities with the nature.

Thus as an intervention to reduce risks associated with climate change induced landslide geohazard, the Department of Geology and Mines (DGM) under Ministry of Economic Affairs (MoEA), Royal Government of Bhutan (RGoB) has carried out the following two key activities under Outcome 1 and Output 1.3 of Second National Adaptation Programme of Action (NAPA-2) Project themed *'Addressing the Risks of Climate-Induced Disasters through Enhanced National and Local Capacity for Effective Actions*, funded by Least Developed Countries Fund (LDCF)-Global Environment Facility (GEF) through United Nations Development Programme (UNDP) and RGoB implementing partner National Environment Commission (NEC) between 2014 and 2017:

1. Integrated geohazard risk assessment and mapping of four critical landslide or landslide affected areas viz.: (1) Moshi landslides and (2) Arong/Lamsorong landslide on Samdrupjongkhar-Trashigang highway; (3) Box-cutting landslide on Gelephu-Zhemgang highway; and (4) Barsa watershed under Phuntsholing Dungkhag, Chukha Dzongkhag; and

2. Landslide monitoring and threshold development of six landslides namely: (1) Moshi landslide, (2) Arong/Lamsorong landslide, (3) Box-cutting landslide, (4) Tshimatsham

Tel: +975-02-322879,323096,323349,323409,324118, Fax: +975-02-323013,326134,324193,339845
P.O.Box No.173, Email:dgm@moea.gov.bt, URL:http://www.moea.gov.bt

དཔལ་ལྡན་འབྲུག་གཞུང་ བསྟན་རྩྭ་ལྟན་ཁག།
ས་རིག་དང་ས་གཏེར་ལས་ཁུངས་ ཐིམ་ཕུག།

Department of Geology and Mines
Ministry of Economic Affairs
Royal Government of Bhutan
Thimphu

on Phuentsholing-Thimphu highway under Chukha Dzongkhag, (5) Reldri landslide under Phuentsholing Thromdey, and (6) Lem landslide, Phongme Geog under Trashigang Dzongkhag.

The goal and objectives of these studies were to: (1) map and assess the four critical landslide affected areas using geo-scientific methods to provide findings and recommendations on suitable mitigation measures (both long term and short term); (2) monitor landslides using geoscientific methods to understand the movement behaviours and record landslide events; (3) develop rainfall thresholds for landslide initiation in the selected monitoring sites; (4) forecast or issue landslide warnings in regions with similar geological and topographical conditions through National Weather and Flood Forecasting and Warning Center (NWFFWC); and (5) share findings and recommendations of these studies with relevant users (national, district, local government, and others) for awareness and importantly for incorporation of the mitigation measures in their plans and implementations for reduction of risks associated with landslide geohazards.

In this regard, DGM on behalf of the Ministry and RGoB is pleased to publish the reports and maps for the four-critical landslide affected areas and six landslide monitoring sites in the country, whose findings and recommendations were shared to the relevant stakeholders during the two-day workshop held at Phuentsholing from 13-14, November 2017.

On behalf of the department, I acknowledge the effort put into publishing these reports and maps and I am hopeful that these documents will be useful to the relevant stakeholders who are responsible in dealing with risks associated with landslide in the study areas.

(Phuntsho Tobgay)
Director General

Tel: +975-02-322879,323096,323349,323409,324118, Fax: +975-02-323013,326134,324193,339845
P.O.Box No.173, Email:dgm@moea.gov.bt, URL:http://www.moea.gov.bt

EXECUTIVE SUMMARY

Moshi area in eastern Bhutan is affected by several landslides that pose a high risk to Samdrupjongkhar- Trashigang national highway and its commuters. As an intervention to climate-induced geologic hazards, the Department of Geology and Mines (DGM) under Ministry of Economic Affairs (MoEA) has carried out integrated geohazard risk assessment and mapping of three landslides in fiscal year 2014-2015 as a part of second National Adaptation Program of Action (NAPA II) Project for climate-change, funded by Least Developed Countries Fund (LDCF) – Global Environment Facility (GEF), coordinated by Bhutan National Environment Commission (NEC) with support from United Nations Development Program (UNDP) under Outcome 1, Output 1.3 of the Project Document. The objectives of this study were: (1) to assess hazards and risks of the three most critical landslides (Landslide-1, 2 and 3), and (2) propose sustainable mitigation measures or solutions to reduce the risks.

This report consists of two parts (Part-I and Part-II). Part-I focuses on large-scale 1:1000 detailed engineering geological mapping and geotechnical survey of the three Moshi landslides. Part-II focuses on Moshi-Tshogoenpa-Lumang watershed hazard and risk assessment using probabilistic and statistical models in GIS.

Detailed engineering geological or geotechnical investigation show that the landslides fall within Shumar Formation of Daling-Shumar Group comprising of thinly bedded quartzite, grey phyllite with quartz boudins and carbonaceous phyllite that are highly deformed with local folding, faulting, shearing, and jointing that has resulted with weak underlying geology in the area. The study area lies within sub-tropical climate zone with relatively high precipitation, where maximum rainfall amount of 3281.2 mm was recorded in 2004 and the minimum rainfall amount of 1555.6 mm was recorded in 2002, between 2000 and 2013. It also shows that the area experiences heavy rainfall from June to September. The maximum rainfall recorded in the area in 2004 is in conformity to the initial landslide event as per locals.

Portable Penetration Test (PPT) results conducted in six pits in the landslide show that the N-Value and corresponding bearing capacity improves from an average depth of 1.11 m with average N-Value of 29. Geotechnical laboratory analysis show that the soils in Moshi area range from poorly graded gravelly sand to well-graded sandy gravel, with C_u ranging from 0.049 to 16.75 and C_c ranging from 0.17 to 12.39; variations in W in soil between 0.56% and 26.38%; and the average coefficient of permeability K value of the soil ranging from 4.45 $x10^{-3}$ cm/sec to 2.80 $x10^{-1}$ cm/sec, indicating fine to coarse-grained sandy soil. The soils in this area also show an average specific gravity of 2.32; average bulk density of 1.69 g/cm^3; average dry density of 1.58 g/cm^3; internal friction angle (ϕ) ranging from 13°29' to 30°57'; cohesion (c) ranging from 0.24 to 0.36 KPa; void ratio (e) ranging from 0.19 to 5.22; porosity ranging from 19.86 to 83.92 %; and degree of saturation (S) ranging from 8.22 to 49.70 %. The Atterberg Limit or Index of Plasticity (PI) average of 23.95% indicate that the soils in the Moshi landslides are highly plastic soil.

The Part-I study concludes that the Moshi landslides are moderately deep-seated and are most likely caused primarily by: (1) weak geology, (2) erratic and heavy precipitation, and (3) steep topography, but aggravated by human activities such as the highway, poor drainage, overgrazing and deforestation. Slope Stability Analyses show that the factor of safety of Moshi Landslide-1 and Moshi Landslide-2 is ~ 0.93 and ~ 0.87, respectively, indicating unstable and slow movement of the slope, and ~ 1.02 for Moshi Landslide-3 indicating stable slope at present.

GIS analysis using Probabilistic and Statistical Models of hazard and risk of landslide in the Moshi-Tshogoenpa-Lumang watershed show three levels of hazard (high, medium and low) as shown in Hazard Map (Plate IV). Two major risks are identified in the area: (1) the Samdrupjongkhar-Trashigang national highway is directly exposed to the landslide hazard. The highway passes right across the two Moshi landslides (Landslide-1 and Landslide 2), where ~300 m of this highway is within the landslide area. Hence, proper planning and implementation of mitigation or remedial measures are necessary to reduce risks to commuters and economy. These landslides also pose high-risk to the

nearby human settlement, where several houses are located nearby or within the landslides and high-risk zone. Detailed engineering geological and geotechnical studies for recommendations of appropriate remedial or mitigations measures especially in medium to high hazard zones are recommended to be carried out prior to construction or development of any infrastructures.

Since both Part-I and Part-II of this study identifies the three Moshi landslides as a high-risk zone, therefore, this report provides specific recommendations on remedial measures or solutions in and around these landslides to reduce risks.

TABLE OF CONTENTS

PART-I
ENGINEERING GEOLOGICAL INVESTIGATION OF THREE MOSHI LANDSLIDES (LANDSIDE-1, 2 &3)

1. INTRODUCTION 1

1.1. OBJECTIVES, OUTPUTS AND OUTCOME OF STUDY 2
1.2. LOCATION AND ACCESSIBILITY OF STUDY AREA 2
1.3. FLORA AND FAUNA 3
1.4. GEOMORPHOLOGY 3

2. REGIONAL GEOLOGICAL SETTING 4

3. METHODOLOGY 6

3.1. DETAILED TOPOGRAPHICAL SURVEY 6
3.2. ENGINEERING GEOLOGICAL AND GEOTECHNICAL INVESTIGATION 6
3.3. LABORATORY ANALYSIS 7
3.4. CLIMATE FACTOR ANALYSIS 7

4. FIELD OBSERVATIONS, RESULTS AND DISCUSSIONS 8

4.1. LOCAL GEOLOGY 8
4.2. ENGINEERING GEOLOGICAL AND GEOTECHNICAL INVESTIGATION 9
4.3. LABORATORY TEST 22
4.4. CLIMATE FACTOR 27

5. DISCUSSIONS AND CONCLUSIONS 29

5.1. MOSHILANDSLIDE-1 (PHOKCHIREY) 29
5.2. MOSHI LANDSLIDE-2 31
5.3. MOSHI LANDSLIDE-3 32

6. RECOMMENDATIONS 36

6.1. MOSHI LANDSLIDE-1 36
6.2. MOSHI LANDSLIDE-2 37
6.3. MOSHI LANDSLIDE -3 37

PART- II
LANDSLIDE HAZARD ASSESSMENT OF MOSHI-TSHOGOENPA-LUMANG WATERSHED UNDER TRASHIGANG DISTRICT, BHUTAN USING PROBABILISTIC AND STATISTICAL MODELS

1. INTRODUCTION 40

2. DATA PREPARATION 41

3. DATABASE CONSTRUCTION FOR LANDSLIDE HAZARD MAPPING 42

4. APPLICATION OF MODELS IN LANDSLIDE HAZARD MAPPING..... 52
4.1. FREQUENCY RATIO 52
4.2. LOGISTIC REGRESSION 58
5. VALIDATION 60
6. RISK ANALYSIS 62
7. DISCUSSION, CONCLUSIONS AND RECOMMENDATIONS..... 63
7. ACKNOWLEDGEMENT..... 63
8. REFERENCES 65

LIST OF FIGURES

Figure 1. Location map of three landslides in Moshi area····· 3
Figure 2. Regional geology of the study area ····· 5
Figure 3 Observation in the pit No. 1.····· 9
Figure 4. Observation in pit No. 2.····· 11
Figure 5. Materials observed in the pit No.3. ····· 12
Figure 6. Materials observation in pit No. 4. ····· 13
Figure 7. Materials observed in the pit No. 5. ····· 14
Figure 8. Observation in pit No. 6.····· 15
Figure 9 - PPT Results from Pit 1 (ZPT).····· 19
Figure 10 - PPT results from pit 2 (PPT). ····· 19
Figure 11. PPT Results from pit 3 (MPT) ····· 20
Figure 12. PPT Results from pit 4 (KPT). ····· 21
Figure 13. PPT Results from pit 5 (LPT).····· 21
Figure 14. PPT Results from pit 6 (TPT).····· 22
Figure 15. Annual cumulative rainfall and average temperature maximum for the year 2000 to 2013 at Wamrong area ····· 28
Figure 16. Structure of GCI.····· 41
Figure 17. Digital elevation model (DEM) and landslide occurrence in the study area ··· 43
Figure 18. Detection of landslide occurrence based on Google satellite imageries. ····· 44
Figure 19. Slope map of the study area.····· 47
Figure 20. Slope length factor of the area.····· 48
Figure 21. Stream power index of the area.····· 48
Figure 22. Topographic wetness index (TWI of the study area).····· 49
Figure 23. Aspect of the study area.····· 49
Figure 24. Plane curvature of the study area. ····· 50

Figure 25. Land use and land cover map of the study area. ····· 50
Figure 26. Distance from road of the study area. ····· 51
Figure 27. Distance from stream of the study area. ····· 51
Figure 28. Work process flow chart of the study area. ····· 54
Figure 29. Cumulative frequency diagram showing landslide susceptibility, index rank occurring in the cumulative percentage of the landslide locations. ····· 62

LIST OF TABLES

Table 1. Pit logging and description of the soil in pit No. 1. 10
Table 2. Pit logging and soil description of pit No. 2. 11
Table 3. Pit logging and soil description in the pit No. 3. 12
Table 4. Pit logging of the soil profile in the pit No. 4. 13
Table 5. Soil profile logging in pit No. 5. 14
Table 6. Logging and description in pit No. 6. 15
Table 7.The relation between N-value and UCS (QU) 18
Table 8. Estimation of allowable Bearing Capacity from N-value 18
Table 9. Results of moisture content. 25
Table 10. The relation between S20 and coefficient of permeability (k) 25
Table 11. The results of Cu, Cc, and Sp. gr 27
Table 12. Computations of Pl, e and S. 27
Table 13. Data layer related to landslide susceptibility analysis 46
Table 14. The relationship between landslide and slope. 55
Table 15. The relationship between landslide and SPI. 56
Table 16. The relationship between landslide and SLF. 56
Table 17. The relationship between landslide and TWI. 56
Table 18. The relationship between landslide and distance from road. 57
Table 19. The relationship between landslide and distance from stream. 57
Table 20. The relationship between landslide and LULC 57
Table 21. The relationship between landslide and curvature 58
Table 22. The relationship between landslide and aspect 58
Table 23. The output of logistic regression analysis 61

LIST OF PLATES

Plate I: Engineering geological map showing proposed mitigation measure of Moshi Landslide-1

Plate II: Engineering geological map showing proposed mitigation measure of Moshi Landslide-2

Plate III: Engineering geological map showing proposed mitigation measure of Moshi landslide-3.

Plate IV: Landslide Susceptibility or Hazard Map of Moshi-Tshogoenpa-Lumang Watershed

PART-I

ENGINEERING GEOLOGICAL INVESTIGATION OF THREE MOSHI LANDSLIDES

(LANDSIDE-1, 2 &3)

1. INTRODUCTION

Slopes are the most common landforms in the Bhutan Himalaya and because of its relatively immature topography, active tectonics, and intense rainfall activities the region is susceptible to landslide incidences. The scenario is further aggravated by unscientific human activities leading to destabilization of slopes. Landslides, as one of the major natural hazards, account for enormous damage to life and property every year. The down-slope movement of masses of rocks, debris or earth under the influence of gravity is termed as a landslide (Cruden and Varnes, 1996).

Moshi area in eastern Bhutan is affected by several landslides that pose a high risk to Samdrupjongkhar- Trashigang national highway and its commuters. This highway is the only lifeline for transportation of foods and goods, business and economic activities for thousands of people living in eastern Bhutan. Therefore, as an intervention to climate-induced geologic hazards, the Department of Geology and Mines (DGM) under Ministry of Economic Affairs (MoEA) has carried out integrated geohazard risk assessment and mapping of three landslides in fiscal year 2014-2015 as a part of second National Adaptation Program of Action (NAPA II) Project for climate-change, funded by Least Developed Countries Fund (LDCF) – Global Environment Facility (GEF), coordinated by Bhutan National Environment Commission (NEC) with support from United Nations Development Program (UNDP) under Outcome 1, Output 1.3 of the Project Document. The fieldwork was carried out for a duration of 75 days.

1.1. OBJECTIVES, OUTPUTS AND OUTCOME OF STUDY

1.1.1. Objectives

The objectives of this study were:

1. to understand the landslide characteristics;
2. determine the causes of the landslides;
3. to assess landslide hazards and risks in and around Moshi landslide affected areas, and
4. propose sustainable mitigation measures or solutions to reduce the risks.

1.1.2. Outputs

The study will generate maps and report that will: (1) help visualize and understand hazard and risks from landslides, and (2) encompass recommendations on mitigation measures or solutions to reduce risks.

1.1.3. Outcome

The end goal is to share findings and recommendations of this study both at a national and local level for: (1) awareness, and (2) mitigation and disaster response planning and implementation to reduce risks of landslide hazards.

1.2. LOCATION AND ACCESSIBILITY OF STUDY AREA

The study area comprising of three critical landslides is located near Moshi village, Lumang Geog, Wamrong Dungkhag under Trashigang District on Samdrupjongkhar–Trashigang national highway in eastern Bhutan (Figure 1) with approximate geographical coordinate 27˚06'44.85" N and 91˚32'38.84" E. The landslides can be accessed on foot from highway, where accessibility to crown and toe of landslide are easy, but body of the landslide is inaccessible due to steep and slippery slope.

Figure 1. Location map of three landslides in the Moshi area (marked as Landslide 1, 2 and 3).

1.3. FLORA AND FAUNA

Moshi area has great varieties of sub-tropical vegetation, which consists of mainly pine-species with bamboos or creepers as undergrowth. Due to geographical location and rain shaded zone, it forms a suitable zone for large varieties of insects, and wild animals like wild-boars, barking deer, wildcats and leopards and a large variety of birds.

1.4. GEOMORPHOLOGY

Series of parallel to sub-parallel gullies and ridges were developed which are mostly oriented all along the major lineaments. Abrupt high standing hillocks/cliffs (Phu) appear to be due to the presence of resistant rocks like the siliceous limestone, quartzite bands and other undisturbed litho-units. Gentle with continuous north facing slope has developed with numerous deep erosion gullies, the reason could be due to deforestation processes as the people practice shifting cultivation in the region, which also contributes substantially to have landslides occurrence. However, shifting cultivation systems has been banned by the Department of Forest and Park Services (DoFPS), Ministry of Agriculture and Forests (MoAF) for the conservation and preservation of natural resources and environments.

2. REGIONAL GEOLOGICAL SETTING

The study area falls within the Shumar Formation of Daling-Shumar Group of rocks under Lesser Himalayan Section (Figure 2). The regional geology in this report is described based on the Geological Map of Bhutan by Long et al., (2011c). The Paleoproterozoic (2500-1600 Ma) Shumar Formation comprise of light coloured, medium to thick bedded (1-2 km except for 6 km thick section local to Kuri Valley) cliff forming quartzite interbedded with thin-thick litho-units of schist and phyllite. This Formation is overlain by Daling Formation with a gradational contact in the North comprising of similar lithologies but dominated by schist and phyllite.

Daling-Shumar Group of rocks are overlain by 600-900 m thick Jaishidanda Formation of the Lesser Himalaya Sequence comprising of Neoproterozoic-Ordovician (?) biotite-rich schist interbedded with quartzite. Further North, the Jaishidanda Formation is overlain by Neoproterozoic-Ordovician rocks of Greater Himalayan Section comprising of paragneiss, schist, quartzite and granitic gneiss intrusive with Main Central Thrust tectonic thrust contact between the two Formations. In the South, Daling-Shumar Group of rocks are underlain by Neoproterozoic-Cambrian[?] lithologies of Manas Formation belonging to Baxa Group, consisting of conglomeratic quartzite interbedded with phyllite and grey dolostone, with contact between them as thrust fault name as the Shumar Thrust.

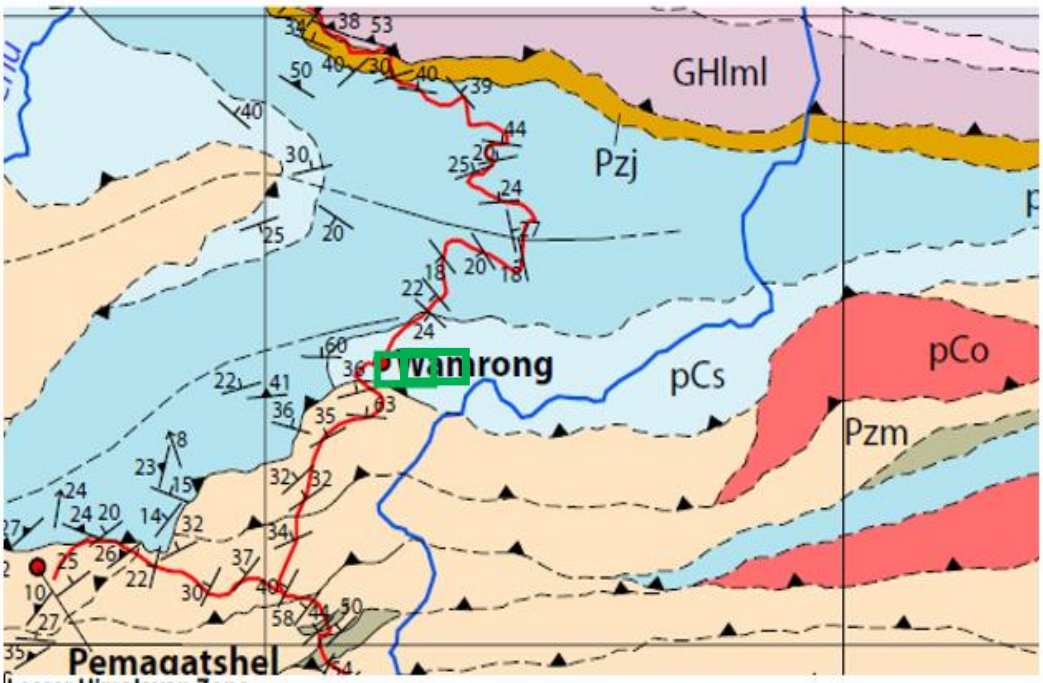

Lesser Himalayan Zone

Pzm / dolo — **Manas Formation*** (Neoproterozoic-Cambrian[?])** - Gray to white, medium- to thick-bedded, medium- to coarse-grained, locally-conglomeratic quartzite exhibiting common trough cross-bedding, interbedded with dark-gray to dark-green, thin-bedded to thinly-laminated phyllite, and medium-gray dolostone (locally divided out) (Bhargava, 1995; Tangri, 1995a; Long et al., 2011A). Intraformational thrust faults indicate structural repetition of multiple, 1.5 to 2.8 km-thick thrust sheets (Long et al., 2011B). Lower greenschist facies (Gansser, 1983).

Daling-Shumar Group (Paleoproterozoic)

pCd — **Daling Formation** - Similar lithologies to Shumar Formation, but dominated by schist and phyllite. Quartzite is thin- to medium-bedded, and medium-gray limestone interbeds are rare. Lower contact is gradational with Shumar Formation (McQuarrie et al., 2008; Long et al., 2011A). Between 2.3 and 3.2 km-thick (Long et al., 2011A).

pCo — **Orthogneiss** - Concordant bodies of mylonitized, granitic orthogneiss at varying stratigraphic levels; interpreted as deformed Paleoproterozoic granite plutons that intruded Daling-Shumar Group (Long et al., 2011A). Thicker in easternmost Bhutan (Gansser, 1983). Interpreted as Indian crystalline basement east of Bhutan in Arunachal Pradesh (Yin et al., 2010).

pCs — **Shumar Formation** - Light-gray to white, tan-weathering, very fine-grained, medium- to thick-bedded, cliff-forming quartzite. Interbeds of thin- to thick-bedded, green, muscovite-biotite schist and phyllite with diagnostic sigmoidal quartz vein boudins become more common upsection. Between 1-2 km thick, except for 6 km-thick section local to Kuri valley (Long et al., 2011A). Upper greenschist facies (Gansser, 1983).

Pzj — **Jaishidanda Formation (Neoproterozoic-Ordovician[?])** – Gray, biotite-rich, locally garnet-bearing schist, interbedded with gray to tan, biotite lamination-bearing, lithic clast-rich quartzite (Bhargava, 1995; Dasgupta, 1995; Long et al., 2011A). Typically 600-900 m-thick, but 1,700 m-thick along Kuri (Long et al., 2011A). Upper greenschist to lower amphibolite facies (Gansser, 1983).

Greater Himalayan Zone

Structurally-lower Greater Himalayan section

GHlo — **Orthogneiss unit (Cambrian-Ordovician)** – Cliff-forming, massive-weathering, granite-composition orthogneiss; generally exhibits leucosomes** and abundant feldspar augen (Long and McQuarrie, 2010; Long et al., 2011B). Paragneiss, schist, and quartzite intervals locally split out. Interpreted as deformed Cambrian-Ordovician granite plutons that intruded Greater Himalayan sedimentary protoliths (Long and McQuarrie, 2010). 1.5-8.0 km-thick; thickens toward eastern Bhutan (Long et al., 2011B).

GHlml — **Lower metasedimentary unit (Neoproterozoic-Cambrian[?])** – Dominantly amphibolite-facies (Gansser, 1983; Grujic et al., 2002; Daniel et al., 2003) metasedimentary rocks, including quartzite, and biotite-muscovite-garnet schist and paragneiss often exhibiting kyanite, sillimanite, or staurolite, and partial melt textures** (Long and McQuarrie, 2010). Orthogneiss intervals locally split out. Up to ~5.0 km-thick; thickens toward western Bhutan.

Figure 2. Regional geology of the study area (Modified after Long et al., 2011c)

3. METHODOLOGY

The following methods were used during this study:

3.1. DETAILED TOPOGRAPHICAL SURVEY

Topographical survey of the study area was carried out using total station TC307 and GPS. The topographical map was prepared in 1:1000 scale with 2 m contour interval using LISCAD and ArcMap software. This map was used as base data/information to prepare, engineering geological map, slope map, land use map, remedial or mitigation measures map, hazard zonation map using ArcMap.

3.2. ENGINEERING GEOLOGICAL AND GEOTECHNICAL INVESTIGATION

Large-scale (1:1000) geological mapping was carried out in and around landslide area to map rock types and structures, and to understand and establish the geological setting of the area. Close-spaced traverses (<10 m) were undertaken; geological points were located using a total station and structural data were recorded using Brunton compass.

Mapping of the material types and mode of depositions was also carried out to determine the type of deposits, which in turn is useful in deducing the geotechnical params of the ground condition.

3.2.1. Pitting

To understand the near-surface soil composition, 6 pits were dug. Visual grain size analysis was done in each pit. Samples were collected for laboratory analysis. A photograph of each pit was also taken. Along the pit profile, different layers were marked and recorded depending on the homogeneity of the layers.

3.2.2. Portable Penetration Test (PPT)

The Portable Penetration Test (PPT) is performed by counting a number of blows required to drive/penetrate the 16 mm diam rod for a length of 10 cm by a free falling 5 kg hammer from a height of 500 mm. The test results were recorded and plotted against the depth to determine the allowable bearing capacity of the ground.

3.3. LABORATORY ANALYSIS

The 12 soil samples collected were analyzed for grain size using sieve analysis method; moisture content; specific gravity; bulk density; porosity; and Atterberg Limit to determine the plastic and *liquid limits* of a fine-grained soil at Geotechnical Laboratory of DGM. The Direct Shear Box Test to determine the shear strength property of soil; and Proctor Compaction Test to determine the soil compaction properties, specifically, to determine the optimal water content at which soil can reach its maximum dry density were carried out at APECS TEST HOUSE-a private engineering consultancy based in Thimphu.

3.4. CLIMATE FACTOR ANALYSIS

The role of climate is important in landslides because climate influences the amount and timing of water, in the form of rain and snow that may infiltrate or erode a hill slope as well as the type and abundance of vegetation that grows on a hill slope. In Bhutan, monsoon (summer months) is the major source of rainfall, where approximately 90% of the total annual precipitation takes place between June and September.

Rainfall and temperature data of Wamrong were collected from Department of Hydro-met Services (DHMS), now National Center for Hydrology and Meteorology (NCHM). The annual rainfall and temperature data from 2000 to 2013 were analyzed using Microsoft Excel.

4. FIELD OBSERVATIONS, RESULTS AND DISCUSSIONS

4.1. LOCAL GEOLOGY

The litho-units encountered in the study area, landslide-1, landslide-2, and landslide-3 during the field investigation are shown in Plate I, II & III respectively and described as follows:

Thinly bedded quartzite

The quartzite is exposed in isolated pockets along the Moshi-Riserboo Highway. It is fine to medium-grained, dirty-white, thinly bedded, highly weathered and fractured with the development of shear planes parallel to the bedding planes. It is exposed in the landslide-1 and landslide 2. The quartzite in the landslide-2 is extremely fractured and pulverized to almost pebble sizes and is highly friable in nature. With the slight touch of the pick of the geological hammer, the wall collapses.

Grey phyllite with quartz boudins

Grey phyllite is found to highly fractured with occasional intercalation of dirty grey-white quartzite and quartz boudins. Quartz veins are frequently found lying concordant to the foliation planes and underlying quartzite.

Carbonaceous phyllite

Carbonaceous phyllite is dark grey to black in colour and at places, it also soils the finger. It is found to be pulverized due to compression most likely because of overlying and underlying competent units. At certain locations, the carbonaceous phyllite appears to be like black clayey material which may be due to shearing. The carbonaceous phyllite zone contains many quartz veins intrusions and mineralized with pyrite, pyrrhotite and magnetite specks.

Geological Structures

The allochthonous rocks of the Daling- Shumar Formation has undergone more than one phases of deformations depicting very complicated geo-structures in the study area. This is mostly represented by numerous small-scale folds, faults and sheared planes, and highly complex litho-succession in the area.

Shumar Thrust forms the major lineament separating the Shumar sequence and Baxa Group of rocks that runs approximately along Nyera Ama course with its corresponding synform and antiform geo-structures (Roy, 1994). Tectonic contact (Shumar Thrust) separating these two Group of Rocks appears to be quite close to the studied site, though the thrust zone trending NE-SW roughly lies near Brekha, Bephu, Thrimsing and Phegpari marked along the Phegpari stream and continues further down along Neyra Ama course. As a result, the rocks of Moshi areas are highly shattered and therefore very prone to landslide occurrences of various magnitudes when combined with the heavy precipitation and other human activities or interventions. The presence of active lineaments passing nearby (Nanung, Moshi and Kharung La fault zone) has created more complications on the slope stability in the area.

4.2. ENGINEERING GEOLOGICAL AND GEOTECHNICAL INVESTIGATION

4.2.1. Soil strata mapping and logging in the pit

a) ***Pit 1- ZPT:*** This pit was dug at Zukpula below girl's hostel, located in the geographical coordinate of N27.132639°, E 91.553247° and at an elevation of 2186 m above the mean sea level. The top parts for about 0.10 m from the surface are greyish brown to slightly dark greyish colluvium and are very loose in nature (Figure 3). This layer is

Figure 3. Observation in the pit No. 1.

underlain by a layer consisting of greyish brown colluvium and clayey soil (Table 1).

Table 1. Pit logging and description of the soil in pit No. 1.

From (m)	To (m)	Total length (m)	Visual estimation for grain size distribution		Soil description
			Particle size	%	
0.00	0.10	0.10	Boulder		Greyish brown to slightly dark grey coloured top soil, loose to very loose in nature.
			Cobble		
			Gravel		
			Sand: Coarse		
			Sand: Medium		
			Sand: Fine		
			Silt		
			Clay		
0.10	1,00	0.90	Boulder		Greyish brown colour of clayey silty soil with the occasional presence of angular pebbles grey phyllite and carbonaceous phyllite. The soil is slightly dense in nature.
			Cobble		
			Gravel		
			Sand: Coarse		
			Sand: Medium		
			Sand: Fine		
			Silt		
			Clay		
1.00	1.80	0.80	Boulder		Dark grey coloured carbonaceous soil with angular cobbles and pebbles of carbonaceous phyllite. The soil is slightly dense in nature. The carb phyllite is underlain by highly fractured grey phyllite.
			Cobble		
			Gravel		
			Sand: Coarse		
			Sand: Medium		
			Sand: Fine		
			Silt		
			Clay		

b) Pit 2-PPT: This pit was dug at Phokcheri, which forms the crown of the Landslide-1, located in geographical coordinate N27.1112˚ and E91.5448˚. The top part for about 0.40 m is greyish brown clayey to silty soil and slightly loose in nature (Figure 4). This

layer is underlain by a layer consisting of greyish brown coloured cobblery, gravelly sand with little fines. The soil is loose and friable in nature mixed with angular boulders, cobbles and gravels of quartzite and phyllite. The detail soil litho logging is presented in Table 2.

Figure 4. Observation in pit No. 2.

Table 2. Pit logging and soil description of pit No. 2.

From (m)	To (m)	Total length (m)	Visual estimation for grain size distribution		Soil description
			Particle size	%	
0.00	0.40	0.40	Boulder		Greyish brown clayey to silty soil with angular boulders, cobbles and gravels of quartzite and phyllite. The soil is slightly loose in density.
			Cobble		
			Gravel		
			Sand – Coarse		
			Sand – Medium		
			Sand – Fine		
			Silt		
			Clay		
0.40	0.70	0.30	Boulder		Greyish brown coloured cobbler, gravelly Silty SAND with little fines. The soil is very loose and highly friable in nature
			Cobble		
			Gravel		
			Sand – Coarse		
			Sand – Medium		
			Sand – Fine		
			Silt		
			Clay		

c) ***Pit 3-MPT:*** This pit was dug on the way towards Moshi Primary School. The top part for about 0.20 m is greyish coloured silty soil (Figure 5). This layer is underlain by 0.40 m thick layer of greyish coloured boulders, densely compacted pebbles and angular fragments of quartzite. The soil is densely compacted (Table 3).

Figure 5. Materials observed in the pit no.3.

Table 3. Pit logging and soil description in the pit No. 3.

From (m)	To (m)	Total length (m)	Visual estimation for grain size distribution		Soil description
			Particle size	%	
0.00	0.20	0.20	Boulder		Grey coloured silty soil loosely compacted.
			Cobble		
			Gravel		
			Sand – Coarse		
			Sand – Medium		
			Sand – Fine		
			Silt		
			Clay		
0.20	1.60	1.40	Boulder	0	Greyish brown coloured, slightly densely as silty clayey soil with occasional presence of angular cobbles and gravels of greyish white coloured, fine-grained quartzite exposed at the bottom.
			Cobble	5	
			Gravel	10	
			Sand – Coarse	20	
			Sand – Medium	15	
			Sand – Fine	15	
			Silt	15	
			Clay	15	
			Boulder		
			Cobble		
			Gravel		
			Sand – Coarse		
			Sand – Medium		
			Sand – Fine		
			Silt		
			Clay		

d) ***Pit 4-KPT:*** This pit was dug at Kheri near ECRD, which is located in geographical coordinate N 27.13202°, E 91.53451°. The top part for about 0.30 m is grey coloured soil consisting of bouldery, cobblery, gravelly sand and silt with the presence of roots (Figure 6). The soil is found to be very loose in nature. This layer is underlain by 1.70 m thick layer consisting of greyish brown coloured cobblery, gravelly sandy silt with clay. The soil is loose in nature with the presence of angular fragments of grey coloured quartzite (Table 4).

Figure 6. Materials observation in pit No. 4.

Table 4. Pit logging of the soil profile in the pit No. 4.

From (m)	To (m)	Total length (m)	Visual estimation for grain size distribution			Soil description
			Particle size		%	
0.00	0.20	0.20	Boulder			Grey coloured silty soil loosely compacted.
			Cobble			
			Gravel			
			Sand	Coarse		
				Medium		
				Fine		
			Silt			
			Clay			
0.20	1.60	1.40	Boulder		0	Greyish brown coloured, slightly densely as silty clayey soil with occasional presence of angular cobbles and gravels of greyish white coloured, fine-grained quartzite exposed at the bottom.
			Cobble		5	
			Gravel		10	
			Sand	Coarse	20	
				Medium	15	
				Fine	15	
			Silt		15	
			Clay		15	
			Boulder			
			Cobble			
			Gravel			
			S	Coarse		
			A	Medium		
			N	Fine		
			D			

e) ***Pit 5-LPT:*** This pit was dug at Lumang located in a geographical coordinate N27.14442˚; E 91. 50119˚.The top part for about 0.50 m is greyish brown sandy topsoil with little fines (Figure 7). This layer is underlain by 1.20 m thick layer consisting of highly to completely weathered quartzite, which is friable in nature. The quartzite has been sheared and pulverized to sandy gravels (Table 5).

Figure 7. Materials observed in the pit No. 5.

Table 5. Soil profile logging in pit No. 5.

From (m)	To (m)	Total length (m)	Visual estimation for grain size distribution		Soil description
			Particle size	%	
0.00	0.50	0.50	Boulder	10	Greyish brown coloured bouldery, cobbler, gravelly sandy top soil with little fines. The clastics consist of angular quartzite and phyllite.
			Cobble	20	
			Gravel	25	
			Sand Coarse	15	
			Sand Medium	15	
			Sand Fine	10	
			Silt	5	
			Clay	5	
0.50	1.70	1.20	Boulder	5	Highly to completely weathered greyish white quartzite which is highly friable and permeable in nature? The quartzite has been shattered and sheared and pulverized to sandy gravels.
			Cobble	10	
			Gravel	35	
			Sand Coarse	20	
			Sand Medium	15	
			Sand Fine	10	
			Silt	5	
			Clay	5	

f) ***Pit6-TPT:*** This pit was dug at Tshogonpa located in a geographical coordinate N 27.11153°; E 91. 49789˚.The top part for about 0.10 m is greyish brown topsoil with the presence of angular fragments of quartzite and carbonaceous phyllite (Figure 8). This layer is underlain by 0.60 m thick layer consisting of grey to ash grey coloured gravelly sand with little fines. The clastic are angular with sharp edges (Table 6).

Figure 8. Observation in pit No. 6.

Table 6. Logging and description in pit No. 6.

From (m)	To (m)	Total length (m)	Visual estimation for grain size distribution		Soil description
			Particle size	**%**	
0.00	2.00	2.00	Boulder	10	Greyish brown coloured bouldery, cobblery, gravelly SAND with little fines. The soil is slightly friable in nature.The clastics are angular in shape with sharp edges and occasionally tabular. The percentage of clastics (coarse materials) increases with depth, and orientation of the clastics are also observed. The clastics are predominantly comprised of greyish-white coloured quartzite.
			Cobble	10	
			Gravel	15	
			Sand – Coarse	20	
			Sand – Medium	20	
			Sand – Fine	15	
			Silt	5	

4.2.2. Engineering Geological Mapping

Moshi Landslide-1

The rocks in the area belong to the Shumar Formation of the Lesser Himalayan Sequence. This Formation is represented by thinly bedded, sheared quartzite with phyllite partings, intercalated with carbonaceous phyllite. The rocks generally strike N30˚E and dip towards NW with dip amount of 44˚-70˚. The shear plane in the area is striking N20˚ E and dip towards NW with dip amount of 40˚. The thickness of shear zone runs with the thickness of 2 m and persistence of 180 m length.

The rock types in this locality is grey coloured, fine to medium-grained, thinly bedded quartzite with thin partings of sheared phyllite. The quartzite is highly to completely weathered and jointed with development of three sets of joints: **J_1-** 070°/84°, J_2-280°/90° and **J_3-**305°/64° The bedding strikes N20°E to N50°E and dips towards NW with dip amount of 44° to 66°and with 0.05 m to 0.15 m wide opened apertures infilled by clayey silt. Numerous shear planes (315°/65°) are developed parallel to the bedding planes. These discontinuities intersect each other weakening the rock mass strength. Numerous water seepages were seen within the body of this landslide, which is one of the main triggering agents for slope instability. The soil is slightly loose in nature. The topsoil layer is underlain by greyish brown coloured cobblery, gravelly SAND with little fines. The soil is friable in nature containing angular boulders, cobbles and gravels of quartzite and phyllite.

Moshi Landslide -2

This landslide observed to be progressing and forming deep gully. Thick, highly friable and permeable, colluvial materials have been observed consisting of angular fragments of quartzite. There is no rock exposed along the road section, however, highly to completely fractured grey quartzite with phyllite partings are seen towards the toe of the landslide. Water seepages are also seen at few places during the study. The soils in

this landslide are very friable and highly permeable in nature, which results in mass movement due to percolation of the rainwater.

Moshi Landslide -3 (lying below the Moshi Primary School)

In this landslide, very thick colluvial materials are observed and no rock is exposed. Predominantly, grey to dark grey phyllite with thin intercalations of quartzite are found exposed at the body of this active landslide. But these rock types are highly weathered, fractured, jointed, crumpled and sheared. Water seepages were seen at few places. The soil is densely compacted. The top part for about 0.20 m is greyish coloured silty soil. This is underlain by 0.40 m thick layer consisting of greyish coloured boulders, densely compacted pebbles and angular fragments of quartzite.

4.2.3. Portable Penetration Test

As laid out in the manual by Sato (2003), different soil parameters, interpretation and classification can be done using PPT results. The relation between "Nc-value" by PPT and "N-value" by Standard Penetration Test (SPT) is given by the following expressions:

$$Nc = (1\text{-}3)\ N$$

However, it is better to use as "Nc =N" because there is a possibility of obtaining a larger value than the actual one in the case of "Nc=3N".

The relation between "N-value "and "soil params" are as follows:

a) Internal Friction angle (Ø)

The following expression is used (in Japan) to estimate "internal friction angle (Ø)" from "N-value:

$$Ø = 15 + 15N^{1/2}$$

b) Uniaxial Compressive Strength (UCS) (q_u)

The relation between "N-value" and "UCS" according to Terzaghi and Peck (1967) is as given in the Table 7:

Table 7.The relation between N-value and UCS (QU) (Terzaghi and Peck 1967).

N	0-2	2-4	4-8	8-15	15-30	>30
$q_{u\ (MPa)}$	<25	25-50	50-100	100-200	200-400	>400

c) Bearing capacity

In the case of construction of bridges or retaining wall (in Japan), an allowable bearing capacity is estimated as shown in Table 8:

Table 8. Estimation of allowable Bearing Capacity from N-value.

Soil Type	**Usually**	**Earthquake**	**N-value**	**Note**
	(KN/m^2)	**(KN/m^2)**		
Sand	300	450	30-50	If N<15 Unit for base.
	200	300	15-30	
Clay	200	300	15-30	
	100	150	8-15	
	50	75	4-8	

PPT1-ZPT

This pit is in the geographical coordinate of N27˚7'57.2" and E91˚33'11.3". In this pit, the 'N' values are very low till the depth of 1 m (Figure 9). After 1 m, the values showed an upward trend. The N values and the corresponding bearing capacity improves at about 1.10 m with the value increasing from 13 to 45, which when calculated gives the bearing capacity ranging from 145 KN/m^2 to 245 KN/m^2 for 2 m width foundation; 118 KN/m^2 to 208 KN/m^2 for 4 m width foundation; and 114 KN/m^2 to 200 KN/m^2 for 6 m width foundation.

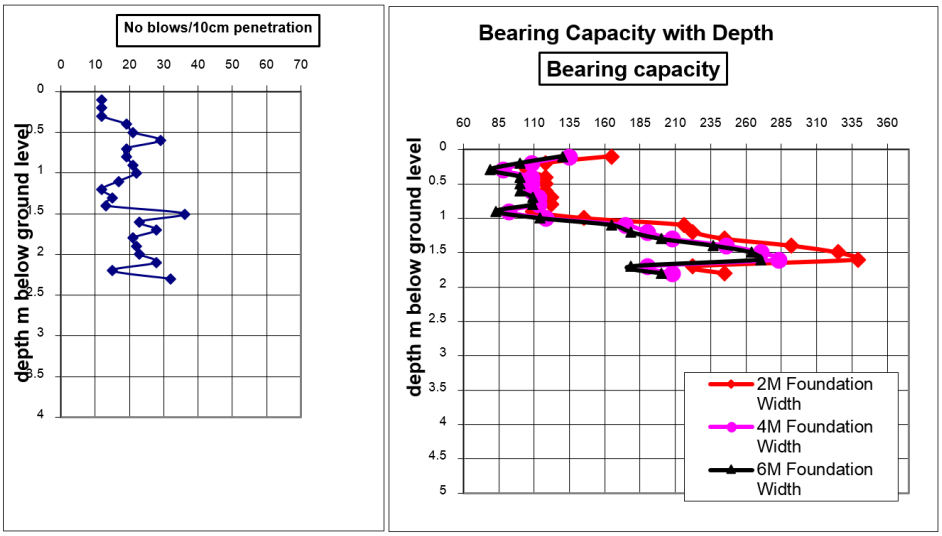

Figure 9 - PPT Results from Pit 1 (ZPT).

PPT2-PPT

This pit is in the Geographical coordinate of N27˚6'40.9" and E91˚32'41.8". In this pit, the 'N' value showed fluctuating results (Figure 10). The 'N' values and the corresponding bearing capacity improves at about 1.5 m with the value of 36, which when calculated gives the bearing capacity ranging from 283 KN/m^2 for 2m width foundation; 234 KN/m^2 for 4 m width foundation; and 225 KN/m^2 for 6 m width foundation.

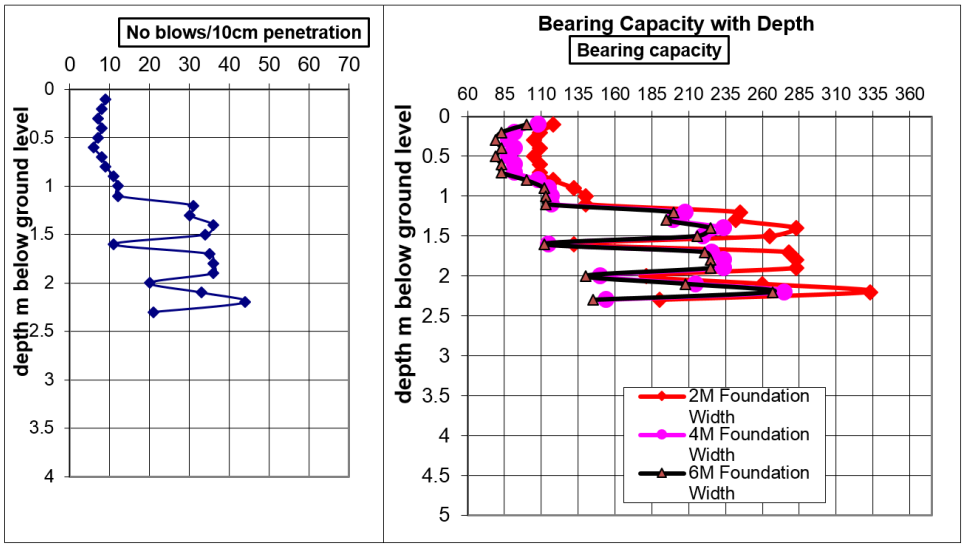

Figure 10 - PPT results from pit 2 (PPT).

PPT3-MPT

This pit is in the Geographical coordinate of N27˚6'41.7" and E91˚31'44.7". In this pit, the 'N' value showed fluctuating results (Figure 11). The 'N' values and the corresponding bearing capacity improves at about 1.7 m with the value of 15, which when calculated gives the bearing capacity ranging from 154 KN/m^2 for 2 m width foundation; 127 KN/m^2 for 4m width foundation; and 122 KN/m^2 for 6 m width foundation. The test was terminated at 2.3 m depth due to the restriction in PPT instrument.

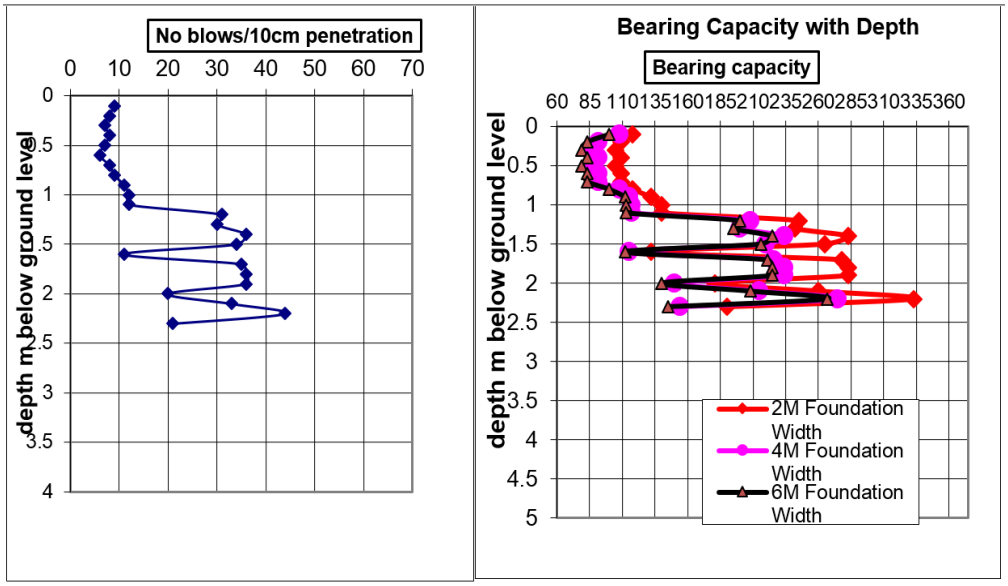

Figure 11. PPT Results from pit 3 (MPT)

PPT4-KPT

This pit is in the Geographical coordinate of N27˚7'54.6" and E91˚32'2.7". In this pit, the 'N' value showed fluctuating results (Figure 12). The 'N' values and the corresponding bearing capacity is maximum at only 0.9 m with the value of 23, which when calculated gives the bearing capacity ranging from 220 KN/m^2 for 2m width foundation; 178 KN/m^2 for 4 m width foundation; and 174 KN/m^2 for 6 m width foundation. The test was terminated at 1 m depth due to the restriction in PPT instrument.

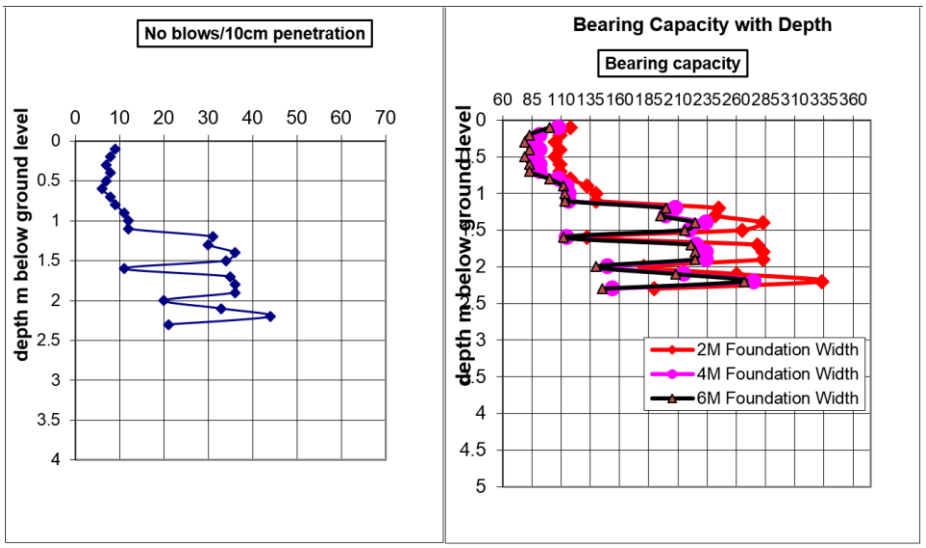

Figure 12. PPT Results from pit 4 (KPT).

PPT-LPT

This pit is in the Geographical coordinate of N27˚6'42.3" and E91˚32'18.9". In this pit, the 'N' value showed fluctuating results (Figure 13). The 'N' values and the corresponding bearing capacity is maximum at only 1.4 m with the value of 36, which when calculated gives the bearing capacity ranging from 283 KN/m^2 for 2 m width foundation; 234 KN/m^2 for 4 m width foundation; and 225 KN/m^2 for 6m width foundation.

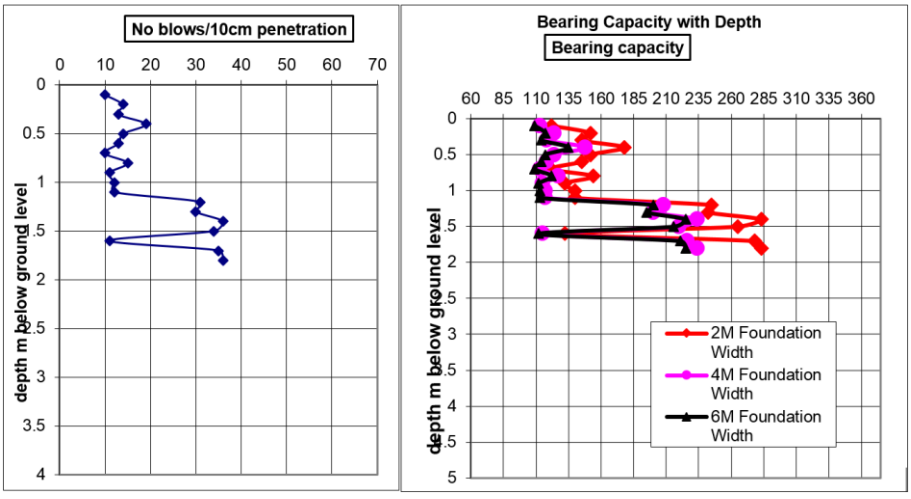

Figure 13. PPT Results from pit 5 (LPT).

PPT6-TPT

This pit is in the Geographical coordinate of N27.11153" and E91.49789". In this pit, the 'N' value showed fluctuating results (Figure 14). The 'N' values and the corresponding bearing capacity is maximum at 0.4 m with the value of 19, which when calculated gives the bearing capacity ranging from 178 KN/m^2 for 2 m width foundation; 148 KN/m^2 for 4 m width foundation; and 135 KN/m^2 for 6 m width foundation. The test was terminated at 0.9 m depth due to the restriction in PPT instrument.

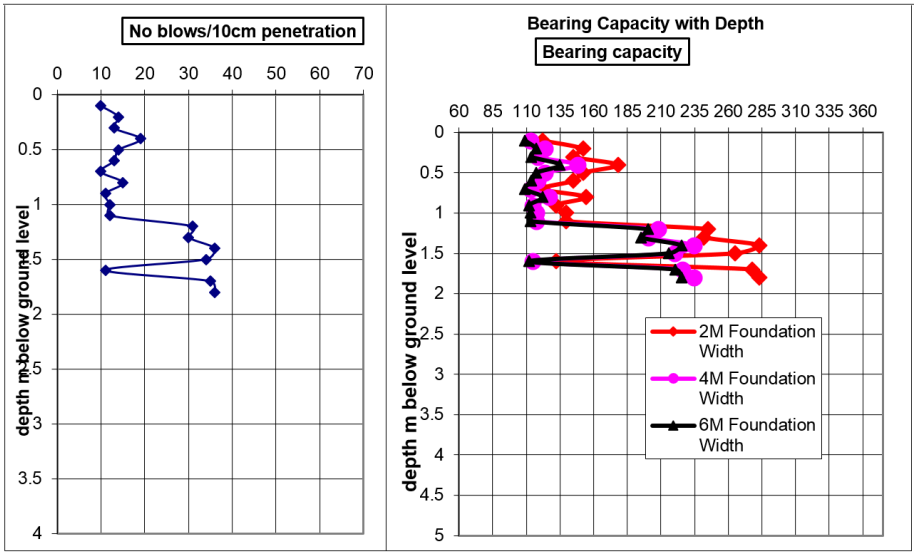

Figure 14. PPT Results from pit 6 (TPT).

4.3. LABORATORY TEST

4.3.1. Sieve Analysis

Sample ZPT-1/1-1 (Pit 1)

The graph plotted using the laboratory sieve analysis data of the sample ZPT-1/1-1 show Gravelly Sand. Using the graph, it is possible to calculate D_{10} and D_{60}, and therefore the Coefficient (C_u) is 5.424 taking D_{10} at 0.895 and D_{60} at 0.895, which shows the gradation of the curve grain size distribution to be wide indicating well-graded soil. The Coefficient

of Concavity (C_c) is calculated using the values of D_{10}, D_{30} and D_{60} and is 0.716. Therefore, the soil does not show a wide range of size since C_c is less than 1. Therefore, it can be considered as poorly graded Gravelly SAND, although its C_u is greater than 5.

Sample PPT-1/1-1 (Pit 2)

The graph plotted using sieve analysis for sample PPT-1/1-1 show Sandy Gravel. Therefore, the character of compaction is poor. Using the graph, it is possible to calculate D_{10} and D_{60} and therefore the C_u is 2 taking D_{10} at 3.45 and D_{60} at 6.9 indicating poorly graded soil. The C_c is calculated using the values of D_{10}, D_{30} and $D_{60}$and is 0.168. Therefore, the soil is poorly graded Sandy Gravel.

Sample MPT-1/1-1 (Pit 3)

The gradation curve or graph plotted using sieve analysis for sample MPT-1/1-1 show Gravelly Sand. The grain size is distributed in less range (uniform soil). Therefore, the character of compaction is poor. Using the graph, it is possible to calculate D_{10} and D_{60}, and therefore the C_u is 4.375 taking D_{10} at 0.160 and D_{60} at 0.7 indicating poorly graded soil. The C_c is calculated using the values of D_{10}, D_{30} and D_{60} and is 0.857. Therefore, the soil is poorly graded Gravelly Sand.

Sample KPT-1/1-1 (Pit 4)

The gradation curve or graph plotted using sieve analysis for sample KPT-1/1-1 show Sandy GRAVEL. The grain size is distributed in less range (uniform soil). Therefore, the character of compaction is poor. Using the graph, it is possible to calculate D_{10} and D_{60}, and therefore the C_u is 0.049 taking D_{10} at 0.150 and D_{60} at 7.3 indicating poorly graded soil. The C_c is calculated using the values of D_{10}, D_{30} and D_{60} and is 0.913. Therefore, the soil is poorly graded Sandy Gravel.

Sample LPT-1/1-1 (Pit 6)

The gradation curve or graph plotted using sieve analysis for sample LPT-1/1-1 show Sandy GRAVEL. The grain size is distributed in a wide range (non-uniform soil). Therefore, the character of compaction is good. Using the graph, it is possible to calculate D_{10} and D_{60}, and therefore the C_u is 12.39 taking D_{10} at 0.251 and D_{60} at 3.11 indicating well-graded soil. The C_c is calculated using the values of D_{10}, D_{30} and D_{60} and is 12.39. Therefore, the soil is well-graded Sandy Gravel.

Sample LPT-1/1-1 (Pit 5)

The gradation curve or graph plotted using sieve analysis for sample TPT-1/1-1 show Sandy GRAVEL. Using the graph, it is possible to calculate D_{10} and D_{60}, therefore, the $C_u$is16.75 taking D_{10} at 0.2 and D_{60} at 3.35, which indicate well-graded soil. The C_c is calculated using the values of D_{10}, D_{30} and D_{60} and is 2.04. Therefore, the soil is well-graded Sandy Gravel.

In general, in the study area, the soils range from poorly graded gravelly sand to well-graded sandy gravel, with C_u ranging from 0.049 to 16.75 and C_c ranging from 0.17 to 12.39.

4.3.2. Moisture content (W)

Soils normally contain a finite amount of water, which can be expressed as the “soil moisture content.” This moisture exists within the pore spaces in between soil aggregates (inter-aggregate pore space) and within soil aggregates (intra-aggregate pore space). Normally this pore space is occupied by air and/or water. If all the pores are occupied by air, the soil is completely dry. If all the pores are filled with water, the soil is said to be saturated. The natural **moisture content** will give an idea of the state of **soil** in the field. The laboratory analytical results of soil samples for the determination of W are provided and its summary is presented in Table 9.

Table 9. Results of moisture content.

Sample No.	ZPT-1/1-1	ZPT-1/2-1	PPT-1/1-1	MPT-1/1-1	KPT-1/1-1	LPT-1/1-1	TPT-1/1-1
Moisture Content	30.22%	13.27%	6.06%	26.38%	21.57%	0.56%	3.74%

Test results show variations in W in soil at Moshi landslide areas between 0.56% and 26.38%. The W differs in even for samples collected from the same pit. For instance, in Pit 1, sample ZPT-1/1-1 collected from 0.9m depth show Was high as 30.22%, whereas, sample ZPT-1/2-1 collected from 0.8m depth show 13.27% W. The higher moisture content shown by samples may relate to the differing rainfall amount during the investigation and during the time of sample collection.

4.3.3. The Coefficient of permeability (K)

The **coefficient of permeability (K)** of a soil describes how easily a liquid will move through a soil. It is also commonly referred to as the hydraulic conductivity of a soil. K can be estimated from the result of sieve analysis. Creager Formula establishes a relationship between K and grain size corresponding to 20% of passing during sieve analysis (D20), which shown in Table 10.

Table 10. The relation between S20 and coefficient of permeability (k) (Creager 1950).

D20(mm)	**K (cm/sec)**	**Soil classification**	**D20 (mm)**	**K (cm/sec)**	**Soil classification**
0.005	$3.00x10^{-6}$	Coarse-grained clay	0.18	$6.85x10^{-3}$	
0.01	$1.05x10^{-5}$	Fine-grained silt	0.20	$8.90x10^{-3}$	Fine-grained soil
0.02	$4.00x10^{-5}$		0.25	$1.40x10^{-3}$	
0.03	$8.50x10^{-5}$	Coarse-grained silt	0.30	$2.20x10^{-3}$	
0.04	$1.75x10^{-4}$		0.35	$3.20x10^{-2}$	
0.05	$2.80x10^{-4}$		0.40	$4.50x10^{-2}$	Medium-grained sand
0.06	$4.60x10^{-4}$		0.45	$5.80x10^{-2}$	
0.07	$6.50x10^{-4}$		0.50	$7.50x10^{-2}$	
0.08	$9.00x10^{-4}$	Extremely fine-	0.60	$1.10x10^{-1}$	

		grained sand			
0.09	$1.40x10^{-4}$		0.70	$1.60x10^{-1}$	
0.10	$1.75x10^{-3}$		0.80	$2.15x10^{-1}$	Coarse-grained sand
0.12	$2.60x10^{-3}$		0.90	$2.80x10^{-1}$	
0.14	$3.80x10^{-3}$	Fine-grained sand	1.0	$3.60x10^{-1}$	
0.16	$5.10x10^{-3}$		2.0	1.80	Fine-grained gravel

For soil sample ZPT-1/1-1, D_{20} grain size or the 20% passing of material from the sieve is at 0.150, which corresponds to K value of $4.45x10^{-3}$ cm/sec. For sample PPT-1/1-1, D_{20} grain size or the 20% passing of material from the sieve is at 0.90, which corresponds to K value of $2.80x10^{-1}$cm/sec. For sample MPT-1/1-1, D_{20} grain size or the 20% passing of material from the sieve is at 0.19, which corresponds to K value of 27.86 $x10^{-3}$ cm/sec. For sample KPT-1/1-1, D_{20} grain size or the 20% passing of material from the sieve is at 0.21, which corresponds to K value of$8.90x10^{-3}$ cm/sec. For sample TPT-1/1-1, D_{20} grain size or the 20% passing of material from the sieve is at 0.5, which corresponds to K value of 7.50x10-^{2} cm/sec.

The average K value of the soil in the Moshi landslide areas range from 4.45 $x10^{-3}$ cm/sec to 2.80 $x10^{-1}$ cm/sec, indicating fine to coarse-grained sandy soil.

4.3.4. Bulk Density (ρ), Dry Density (ρ_d), Angle of internal friction(Ø), Cohesion (C), Specific Gravity (Sp. Gr), Porosity (η), Void Ratio (e), Degree of Saturation (S), Index of Plasticity.

The laboratory analytical results of soil samples for determination of Bulk Density (ρ), Dry Density (ρ_d), Angle of internal friction(Ø), Cohesion (C), Specific Gravity (Sp. Gr), Porosity (η), Void Ratio (e), Degree of Saturation (S), Index of Plasticity summarizations are presented in Tables 11 and 12.

Table 11. The results of Cu, Cc, and Sp. Gr.

Sample No.	Gradation curve from sieve analysis				Direct Shear Box		Bulk and Dry Density		Specific Gravity
	Dry		Wet		ϕ	C (KPa)	ρ (g/cm^3)	ρd (g/cm^3)	Sp. Gr
	Cc	Cu	Cc	Cu					
LPT-1/1-1	1.037	12.39	2.344	10.667	-	-	1.83	1.81	2.33
PPT-1/1-1	0.168	2.00	1.99	9.178	18°26`	0.32	1.78	1.67	2.43
ZPT-1/1-1	0.716	5.424	0.498	29.44	23°57`	0.24			2.26
ZPT-1/2-1	1.257	14.865	2.00	12.5	21°48`	0.32			2.37
MPT-1/1-1	0.857	4.375	0.575	16.667	14°55`	0.28	1.33	1.05	2.36
KPT-1/1-1	0.913	0.049	0.453	9.483	13°29`	0.36			2.12
TPT-1/1-1	2.043	16.75	-	-	30°57`	0.3	1.83	1.77	2.4

Table 12. Computations of Pl, e and S.

Sl. No.	Sample No.	Atterberg Limit			Void ratio (e)	Porosity (η) (%)	Degree of saturation (S) (%)
		Liquid Limit (W_L) (%)	Plastic Limit (W_P) (%)	Index of Plasticity (PI) (%)			
1.	LPT-1/1-1	-	-	-	0.249	19.857	8.217
2.	PPT-1/1-1	-	-	-	0.457	31.359	35.393
3.	ZPT-1/1-1	67.9	41.79	26.11	5.218	83.919	12.965
4.	ZPT-1/2-1	47.04	27.96	19.08	5.079	83.549	8.406
5.	MPT-1/1-1	61.20	34.08	27.12	0.19	55.5	49.7
6.	KPT-1/1-1	54.77	31.28	23.49	1.132	53.098	41.72
7.	TPT-1/1-1	-	-	-	0.36	26.71	21.58

4.4. CLIMATE FACTOR

Climate can be defined as the characteristic weather at a place or region over seasons, years or decades. The role of climate is important in landslides because climate influences the amount and timing of water, in the form of rain and snow that may infiltrate or erode a hill slope as well as the type and abundance of vegetation that grows on a hill slope. Climate plays a very important role in the process of weathering and erosion, which is related to the stability of the slopes. Rain in many cases trigger

landslides and drastic changes in diurnal temperature speed up the process of weathering.

The studied area falls in the sub-tropical climate zone with warm to hot summer and pleasant to cold winter. Monthly cumulative rainfall data and average maximum temperature from 2000 to 2013, collected by National Center for Hydrology and Meteorology (NCHM) for Wamrong area (an area near to Moshi landslides) are presented in Figure 15. The annual cumulative rainfall amount and maximum temperature are presented in Figure 15. These records show variations in both monthly and annual rainfall and maximum temperature, where maximum rainfall amount of 3281.2 mm was recorded in 2004 and the minimum rainfall amount of 1555.6 mm was recorded in 2002. It also shows that the area in and around study area experiences heavy rainfall from June to September and remains dry in autumn and spring.

According to the local people, landslides at Moshi were initiated in 2004, which is in conformity to the highest annual rainfall recorded between 2000 and 2013. This indicates that rainfall is one of the major triggering factors of landslides in the Moshi area.

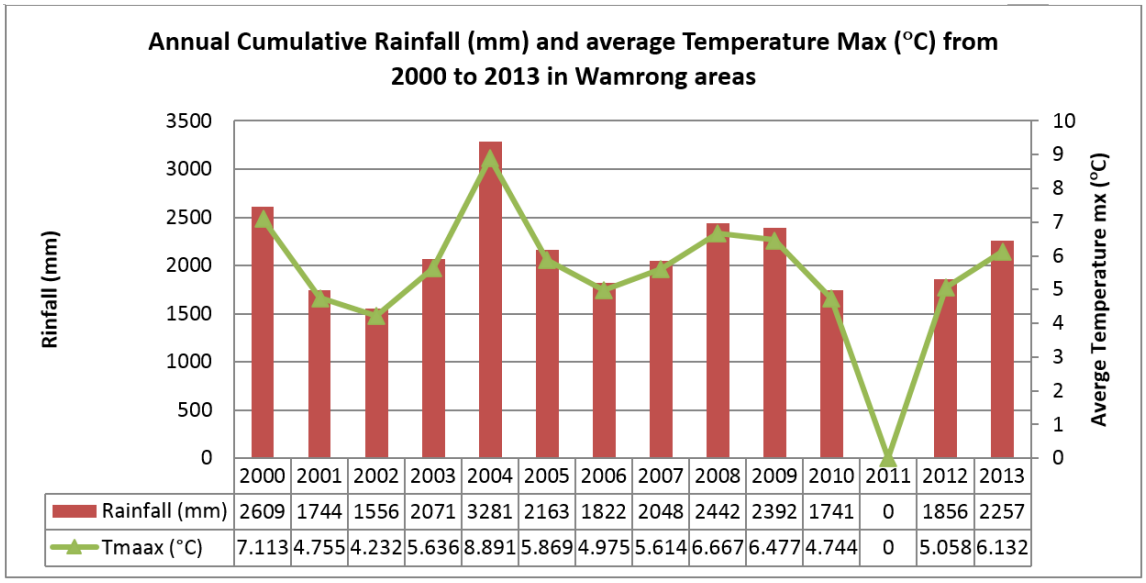

	2000	2001	2002	2003	2004	2005	2006	2007	2008	2009	2010	2011	2012	2013
Rainfall (mm)	2609	1744	1556	2071	3281	2163	1822	2048	2442	2392	1741	0	1856	2257
Tmaax (°C)	7.113	4.755	4.232	5.636	8.891	5.869	4.975	5.614	6.667	6.477	4.744	0	5.058	6.132

Figure 15. Annual cumulative rainfall and average temperature maximum for the year 2000 to 2013 at Wamrong area (NCHM).

5. DISCUSSIONS AND CONCLUSIONS

5.1. MOSHILANDSLIDE-1 (PHOKCHIREY)

5.1.1. Material type

This landslide was propagating rapidly upslope, which has a more than 10 m slip face angle with the development of multiple tension cracks above the crown. This is one of the very active landslides with a complex phenomenon. The rock types in this locality are grey coloured, fine to medium-grained, thinly bedded quartzite with thin partings of sheared phyllite. The quartzite is highly to completely weathered and jointed with the development of three sets of joints and they are **J_1-** 070°/84°, J_2- N80°W/90° and **J_3-** 305°/64°. The quartzite bedding strikes N20°E to N50°E and dips 44° to 66° towards NW with 5 cm to 15 cm wide open spaces or apertures infilled by clayey silt. Numerous shear planes (315°/65°) were found to have developed parallel to the bedding planes. These discontinuities have been found to intersect each other weakening the rock mass strength. Numerous water seepages are seen within the body of this landslide.

5.1.2. Causes of the landslide

The following factors appear to be the main triggering factors or causes of the landslide in Moshi Landslide-1 area:

(1) Toe scouring by the prolonged and heavy precipitation during the monsoon.

(2) Easy infiltration of the rainwater into the highly crumpled phyllite zone and gradually making their avenues like reel and gullies to erode the phyllite down valley.

(3) Downhill throwing practices of excavated materials (muck) during the road blockage, which eventually increases its load due to heavy and prolonged precipitation. The overburden soils are porous and permeable in nature, which allows the rainwater infiltration causing the decrease of shear strength of soil

and highly crumpled phyllite adding the weight due to saturation and thereby leads to mass movement.

5.1.3. Slope Stability Analysis

Considering the landslide as a moderately deep-seated slide, the Modified Bishop's method is applied to estimate the factor of safety. Modified Bishop's method is slightly different from the ordinary method of slices in that normal interaction forces between adjacent slices are assumed to be collinear and the resultant interstice shear force is zero. The constraint introduced by the normal forces between slices makes the problem statically indeterminate. As a result, iterative methods must be used to solve for the factor of safety (Donald et. al., 2011)

The factor of safety for moment equilibrium in Bishop's method can be expressed as

$$F = \frac{\sum_j \frac{[c' l_j + (W_j - u_j l_j) \tan \phi']}{\psi_j}}{\sum_j W_j \sin \alpha_j}$$

where

$$\psi_j = \cos \alpha_j + \frac{\sin \alpha_j \tan \phi'}{F}$$

Where,

j is the slice index,

c' is effective cohesion,

Ø' is effective internal friction

l is the width of each slice

W is the weight of each slice

μ is water pressure at each base.

In Moshi Landslide-1, we assumed the landslide is rotational slide and the rapture surface is located varying from 1m to 30m depth. The angle for each slice is found to be about 3 to 65 degree. The frictional angle is calculated to be about 35^0. The bulk unit density is found to be about 21.37 KN/m^3 with the cohesion of about 4 KN/m^3. Since the water is observed to be seeping out at toe of the slide, hence the rupture surface is assumed to be located at deeper depth. The thickness of each slice varies from about 1 to 30 m. After analyzing the slope stability in the area, the factor of safety is calculated about 0.93, which is less than one. This indicates that slope is not stable and moving at a slow rate.

5.2. MOSHI LANDSLIDE-2

5.2.1. Material type

This landslide was progressing forming deep gully. Thick colluvial materials have been observed having angular fragments of quartzite and these colluvial materials are highly friable and permeable in nature. No rock exposure is seen along the road section. However, highly to completed fractured grey quartzite with phyllite partings are seen towards the toe of the landslide. Water seepages are also seen at few places.

5.2.2. Causes of the landslide

The following factors appear to be the main triggering factors or causes of the landslide in Moshi Landslide-2 area:

(1) Due to the formation of deep gully resulting collapse of the loose to very loose colluvial soil. These soils are very friable and highly permeable in nature, which results in mass movement due to percolation of the rainwater.

(2) Conventional practices of throwing the muck downhill during road blockage, which adds the weight under saturated condition.

(3) Lack of drainage along this landslide stretch.

(4) Very high slip face angle of the landslide at its crown.

5.2.3. Slope Stability Analysis

This landslide is classified as a shallow landslide, which means the depth of the slide is shallow (10-20 m). In this kind of slide, we applied limit equilibrium analyses. In the limit equilibrium analyses, we evaluate the slope as if it were about to fail by sliding with a well-defined body of the slide at limiting equilibrium and determine the resulting shear stress along the well-defined failure surface. Then this shear stresses are compared to that of the cross-ponding shear strengths to determine the factor of safety. The formula used for determining the factor of safety is shown below.

$F = S/S'$

Where, F is factor safety

S is the shear strength

S' is the shear stress

In this landslide, we assumed the landslide is translational slide and the rupture surface is located fairly at shallow depth about an average of 10 m. The slope angle is about 55^0. The frictional angle is calculated to be about 35^0. The bulk unit density is found to be about 21.37 KN/m^3 with the cohesion of about 4 KN/m^3. After analyzing the slope stability in the area, the factor of safety is calculated about 0.87, which is less than one. This indicates that the slope is not stable and moving at a slow rate.

5.3. MOSHI LANDSLIDE-3

5.3.1. Material type

This landslide is also widening on its both flanks forming deep gully. There are very thick colluvial materials observed where no rock is exposed. Predominantly, grey to dark grey phyllite with thin partings of quartzite that are highly weathered, fractured, jointed,

crumpled and sheared are found exposed at the body of this landslide. Water seepages are seen at few places.

5.3.2. Causes of the landslide

The uneven ground surface right below the Moshi Primary School is the indication of mass movement/slope instability. The slope angle increases towards the toe of the landslides. The following factors appear to be the main triggering factors or causes of the landslide in Moshi Landslide-3 area:

(1) Uncontrolled sewerage water from the school compound.

(2) Overgrazing and cutting down of the trees/plants.

(3) Very friable and highly permeable nature of the soil. However, the crown portion of this landslide is deduced to be dormant now due to the growth of plants and undergrowth.

(4) No drainage was maintained along this landslide stretch.

(5) No major remedial measures were put in place, except few bamboos were seen to be planted recently by the school management.

(6) Weak underlying geology characterized by thinly laminated and flaggy quartzite that is highly weathered, sheared and fractured/jointed with the development of numerous joints/shear planes and phyllite is sheared, crumpled and decomposed to gravelly clay. One of the prominent shear zones is found to run from above the Zugpola Higher Secondary School to North of Kheri village. The second prominent shear zone traverses from Kosphu villages and passes through the Moshi (Phockchirey) Landslide No. 1. The third major one runs SE of 90 km milestone (Samdrupjongkhar-Trashigang Highway) and merges with active landslide lying below Moshi Primary School. The shear zone follows the bedding/ foliation of quartzite and phyllite.

(7) Presence of thick (at some places > 8 m) highly friable and permeable colluvial materials comprising of angular fragments of quartzite with a negligible amount of cementing matrix in and around this landslide.

5.3.3. Slope Stability Analysis

This landslide is classified under a shallow landslide, which means the depth of the slide is shallow. In this kind of slide, we applied limit equilibrium analyses to determine the factor of safety. The formula used for determining the factor of safety is shown below.

$F = S/S'$

Where, F is the factor safety

S is the shear strength

S' is the shear stress

In this landslide, we assumed the landslide is translational slide and the rapture surface is located fairly at shallow depth about an average of 5 to 10 m. The slope angle is about 45^0. The frictional angle is calculated to be about 21^0. The bulk unit density is found to be about 21.37 KN/m^3 with cohesion of about 4 KN/m^3. After analyzing the slope stability in the area, the factor of safety is calculated about 1.02, which is more than one. This indicates that the slope is stable now.

In general, in the Moshi area, the landslides were most likely caused by:

(1) Erratic heavy rainfall as observed during 2004.

(2) Weak underlying geology comprising mainly of grey to carbonaceous phyllite and thinly bedded flaggy quartzite belonging to the Shumar Formation of Paleoproterozoic age which are highly weathered, fractured/jointed, and sheared possibly due to its proximity to the Shumar Trust.

(3) Steep topography and presence of thick highly friable and permeable colluvial materials.

(4) Human interaction through highway construction with poor maintenance of drainage, deforestation taken place in the past from shifting cultivation, and overgrazing by domestic animals.

6. RECOMMENDATIONS

Based on the findings and conclusions of this study, the following mitigation or remedial measures in and around three Moshi landslides are proposed. The proposed remedial measures are shown on the Engineering Geological Maps showing Proposed Mitigation Measure of Moshi Landslides (Plate I-III).

6.1. MOSHI LANDSLIDE-1

(1) Catch drain/garland drain should be constructed on top of the crown of this active landslide.

(2) Cement lining of the side drain along the road should be done and safely disposed of.

(3) The tension cracks must be filled by fine materials and stemmed properly to avoid infiltration of the surface runoff during heavy precipitation.

(4) Check dams and gabion retaining structures are recommended to construct.

(5) Sandbags (coarse sand and gravel) may be used as retaining wall.

(6) Water seepages from the landslide areas are to be properly collected and safely disposed to downslope preferably to the natural gully or depressions.

(7) Sub-horizontal perforated either HDPE Pipe or perforated NX casing should be in place for drawing the sub-surface water from the landslide.

(8) Bio-engineering with suitable species of trees/plants and grasses should be done just before the onset of monsoon.

(9) Cutting down of trees/plants and overgrazing should be prohibited in these areas.

(10) Landscaping of the slope in 1:2 (Vertical: Horizontal) ratio will help in reduction of slope instability to some extent.

(11) Application of suitable geotextile method should be adopted especially where soil cover is thick.

6.2. MOSHI LANDSLIDE-2

(1) Catch drain/garland drain should be constructed on top of the crown of this active landslide.

(2) Cement lining of the side drain along the road should be done and safely disposed of.

(3) The tension cracks be filled by fine materials and rammed properly to avoid infiltration of the surface runoff during heavy precipitation.

(4) Check dams along the depressions should be constructed to avoid bed incision and gabion retaining structures are recommended to construct.

(5) Sandbags with coarse gravels may be used as retaining wall.

(6) Water seepages from the landslide areas are to be properly collected and safely disposed to downslope preferably to the natural gully.

(7) Sub-horizontal perforated either HDPE Pipe or perforated NX casing should be in place for drawing the sub-surface water from the landslide.

(8) Bio-engineering with suitable local species of trees/plants and grasses should be planted before the onset of monsoon.

(9) Cutting down of trees/plants and overgrazing should be restricted in these areas.

(10) Landscaping of the slope in 1:2 (Vertical: Horizontal) ratio will help in reduction of slope instability to some extent.

(11) Application of suitable geotextile method should be adopted especially where soil cover is thick.

6.3. MOSHI LANDSLIDE -3

(1) Deep catch drain/garland drain should be constructed right from the edge of the football ground and safely disposed to natural gully.

(2) Series of French drains may be constructed just below the football ground and connected to main depression.

(3) The tension cracks be filled by fine materials and rammed properly to avoid infiltration of the surface runoff during heavy precipitation.

(4) Gabion check dams/sandbags check dams may be constructed along the deep gullies to avoid bed incision.

(5) Flexible structures such as gabion retaining walls are recommended to construct.

(6) Water seepages from the landslide areas are to be properly collected and safely disposed to downslope preferably to the natural gully.

(7) Sub-horizontal perforated either ~~HD~~HDPE Pipe should be in place for drawing the sub-surface water from the landslide.

(8) Bio-engineering with suitable local species of trees/plants and vetiver grass *Chrysopogonzizanioides* should be planted before the onset of monsoon.

(9) Cutting down of trees/plants and overgrazing should be restricted in these areas.

(10) Landscaping of the slope in 1:2 (Vertical: Horizontal) ratio will help in reduction of slope instability to some extent.

(11) Application of suitable geotextile method should be adopted especially where soil cover is thick.

PART- II

LANDSLIDE HAZARD ASSESSMENT OF MOSHI-TSHOGOENPA-LUMANG WATERSHED UNDER TRASHIGANG DISTRICT, BHUTAN USING PROBABILISTIC AND STATISTICAL MODELS

1. INTRODUCTION

GIS is currently used in the geosciences, but it is also applicable for other fields of research and can be applied to such topics as the environment, civil and urban engineering, agriculture, forestry, business, military, government, and educational research and applications. There are no limitations to the use of GIS, and it is constantly expanding into new areas. In this probe, we confine our focus to applications in the geosciences, that is, geological hazards.

GIS is an information technology that has transformed geoscience research by aiding in the analysis of geospatial data and by producing information more efficiently than traditional techniques. GIS also serves an important role as an integration technology because it can create susceptibility or potentiality maps for many fields of geoscience, including studies of natural hazards, geological resources, environments, and ecosystems. In the past, the creating of such maps was considered laborious and time-consuming, but this process is now comparatively easy because of significant advances and developments in GIS technology. Geospatial Correlation Integration (GCI) is similar in concept to the overlay function which is a core concept of GIS technology; however, GCI is a more comprehensive and detailed technique. GIS-based GCI has been widely used in modelling applications in the geosciences, and its applications and modelling capabilities are unlimited.

The structure of GCI is shown in Figure 16. Spatial data used for GCI can be divided into two types: dependent data and independent data. The data are integrated to generate susceptibility and potential maps using expert-opinion, probabilistic, statistical, and data mining models (Lee, 2012)

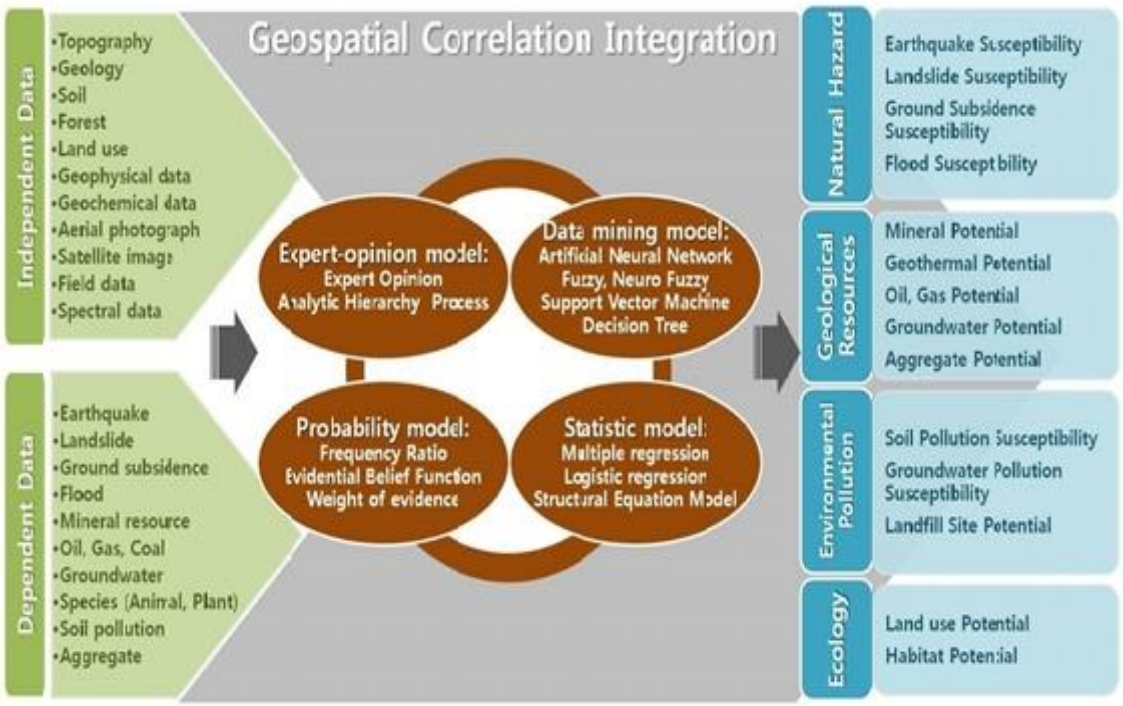

Figure 16. Structure of GCI.

2. DATA PREPARATION

To generate susceptibility/hazard maps, complete and comprehensive data preparation is of supreme significance. The point is each geo-scientific event results from different causes. The data preparation process must include a complete understanding of the features of the probe area and source data that defines the dependent and independent factors at the time of the construction of databases. For example, flood susceptibility is governed by many hydrological factors, such as surface and slope steepness and morphology, stream evolution, climate, soil, vegetation cover, land use, bedrock lithology, structure and human activity. However, macrobenthos habitat is significantly dependent on temperature conditions created by exposure duration and the intertidal elevation. This chapter discusses the data preparation or construction of databases for the landslide susceptibility or hazard mapping.

3. DATABASE CONSTRUCTION FOR LANDSLIDE HAZARD MAPPING

Many studies have been carried out to assess landslide susceptibility/hazard with the application of GIS and different models. Many of those studies have applied probabilistic models such as frequency ratio and weight of evidence. (Lee and Min, 2001; Lee et al., 2004a; Lee and Pradhan, 2006; Dahal et al., 2008; Audisio et al., 2009; Mousavi et al., 2009; Oh et al., 2009; Ozdemir, 2009; Pirasteh et al., 2009; Pradhan and Youssef, 2009; Vahidnia et al., 2009; Yalcin, 2008; Yilmaz, 2009a, b; Regmi et al., 2010; Yilmaz, 2010; Yalcin et al., 2011). One of the statistical models available, the logistic regression model, has also been applied to landslide susceptibility mapping (Lee, 2005, 2007a; Akgun and Bulut, 2009).

In some researches, landslide-hazard analysis techniques have been cross-applied and validated (Oh and Lee, 2010c; Pradhan and Lee, 2010a; Pradhan et al., 2010a). For the same studies, Park and Lee (2014) the frequency ratio and logistic regression models have been applied and compared. In this study, the spatial database was constructed according to the research of Park and Lee (2014).

In the study area of Moshi-Tshogoenpa-Lumang watershed under Trashigang District, landslides are common during the summer or rainy season. Moshi area suffers from recurring and extensive damage from the landslides. Given its vital economic link in eastern Bhutan, the area was identified for investigation.

Geologically, the area falls under the Shumar formation, where light-grey to white, tan weathering, very fine-grained, medium to thick-bedded, cliff-forming quartzite are the prominent features. Inter-beds of thin to thick bedded green, muscovite-biotite schist and phyllite with diagnostic sigmoidal quartz vein boudins mostly 1-2 km thick, except 6km thick local to Kuri valley (Long et al., 2011a) which becomes more common up section (Gansser, 1983) are some of the other geological characteristics.

The Moshi area of Trashigang District experiences sustained yearly damage from the landslides, resulting in the cut off in road communication link and agricultural land

losses. The circular black dots represent areas in which landslides have occurred (verified during fieldwork, 2015). Satellite imageries from Google provide pictures of landslides, and visual interpretation of satellite imageries/Aerial Photography combined with field surveys has been the main approach to landslide inventory mapping until recently (Kääb, 2002; Casson et al., 2003; Martha et al.,2010). In this study, for the detection of landslide locations, digital satellite imageries from Google were retrieved from the Google earth (Figure 17).

The high-resolution photographs/ satellite imageries are preferred. In the absence of latest and high-resolution aerial photographs and satellite imageries, Google earth imageries were employed. To ascertain the accurate landslide locations, which was visually detected and interpreted from the Google earth imageries, an extensive field investigation was carried out (Figure 18).

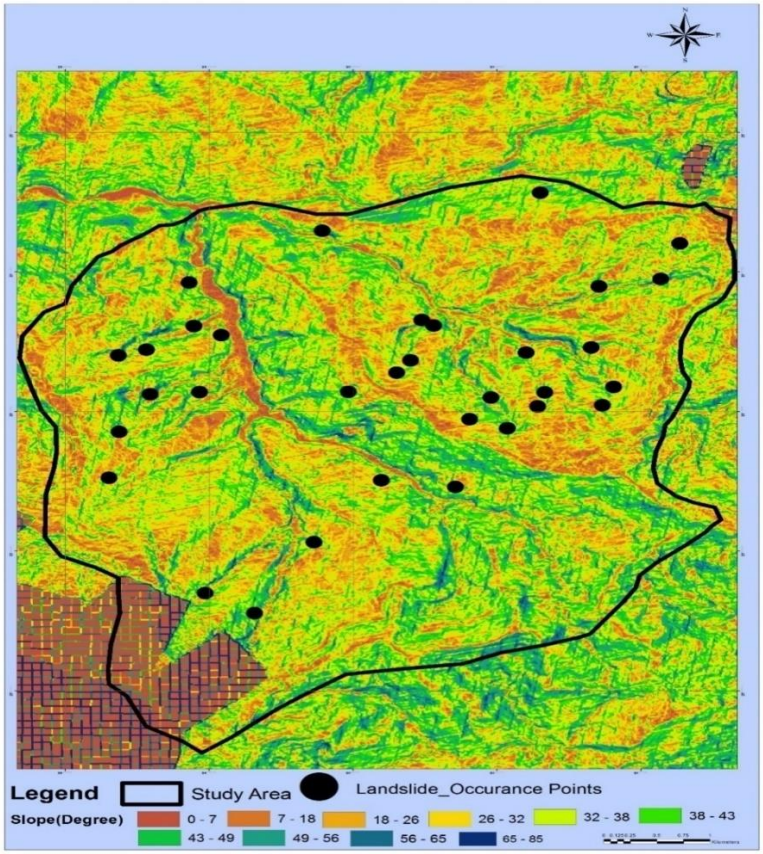

Figure 17. Digital elevation model (DEM) and landslide occurrence in the study area.

Figure 18. Detection of landslide occurrence based on Google satellite imageries.

In the study area, rainfall-triggered shallow soil slides and debris flows are abundant. Most landslides have approximate lengths between 200 and 500 m, widths between 20 and 150 m, and depths less than 30 m. The landslides were mapped as initiation points, and the total number of landslides in the case study areas was 70. The location of each landslide was denoted by a pixel of 10 m × 10 m and is shown in Figure 17. The landslide data were randomly divided into training data (50% of landslide locations: 35 landslides) and validation data (50% of landslide locations: 35 landslides).

Landslides result from the interaction of complex factors, so the selection of factors and preparation of corresponding thematic data layers are crucial for models that create landslide-susceptibility/hazard mapping (Sarkar and Kanungo, 2004). In general, the instability factors for landslides include lithology, geological structures, seismicity, slope steepness, morphology, stream evolution, groundwater conditions, climate, vegetation cover, land use, and human activity.

This study considered topography, geology, land use, forest, and soil factors, which were collected from available maps and in-field investigations and are listed in Table

13. A digital elevation model (DEM) was clipped into the Area of interest (AOI) from the ALOS-prism DEM. Using the DEM, the slope gradient (Figure 19), slope length (Figure 20), stream power index (SPI) (Figure 21), topographic wetness index (TWI) (Figure 22), slope aspect (Figure 23), and plan curvature (Figure 24) were calculated. The geological, Land Use and Land Cover map, and Lineament maps are provided in polygon coverage with scales of 1:50,000, 1:250,000, and 1:25,000, respectively, and two of the maps were published by DGM and the Land Use and Land Cover map (Figure 25) by MoAF, respectively.

The maps relevant to landslide occurrence were constructed in a vector format spatial database using the ArcGIS (ESRI) software package. Eight factors, both calculated and extracted from the maps, were converted to a 10 m × 10 m grid format (ArcGIS GRID type). As a result, the dimensions of the case study area grid were 502 rows by 607 columns, so the total number of cells was 3, 04,714. To calculate the frequency ratio and Logistic Regression for the class or type of each factor, the scale factors were divided into ten classes based on the equal area using ArcGIS. Therefore, the range of each class was automatically determined based on an equal area.

The topographic factors reflect the geomorphological characteristics of the investigation area. The slope gradient, slope aspect and plan curvature can influence landslide initiation (Dai and Lee, 2002), and the topography has a vital role in the spatial variation of hydrological conditions such as soil moisture, groundwater flow and slope stability. Topographic indices are used to describe the spatial soil moisture patterns (Moore et al., 1991), and the SPI measures the erosion power of streams and is also considered as a factor contributing towards the stability within the case study area.

Table 13. Data layer related to landslide susceptibility analysis (Park and Lee, 2014).

Category	Factors	Data Type	Scale
Geological hazard map	Landslide	Point	
Topographic map	Slope gradient Slope aspect Curvature TWI SPI Distance from lineament	GRID	1:50,000
Geological map	Geology	Polygon	1:250,000
Land use map	Land use	Polygon	1:250,000

The SPI can be defined as follows (Moore et al., 1991):

$$SPI = A_s \tan \beta,$$

Where A_s is the area of the specific catchment and β is the local slope gradient measured in degrees.

Another topographic factor within the run-off model is the TWI (Beven and Kirkby, 1979), defined as follows:

$$TWI = \ln (\alpha / \tan \beta)$$

where α is the cumulative upslope area draining through a point (per unit contour length) β is the slope angle at the point and ln (α/tan β) is an index reflecting the tendency of water to accumulate at any point in the catchment (in terms of α) and gravitational forces to move that water down the slope (expressed in terms of tan β as an approximate hydraulic gradient). The water infiltration primarily depends upon material properties such as permeability and pore water pressure and their effects on the soil strength.

Lithology plays an important role in landslide occurrences because lithology units can have different inherent characteristics, such as compactness, composition and structure that produce varied resistance against landslides (Carrara et al., 1991; Kincal et al., 2009; Chauhan et al., 2010). Faults as a geological structural are the surface expression of buried features and structures. The fault describes the plane of weakness and tectonic activity along which the landslide susceptibility is higher.

The occurrence of landslides varies with the land-use pattern, which is an indication of the stability of hill slopes (Anbalagan, 1992). The params of forest and soil affect various geomorphologic processes, including the enhancement of surface erosion, change of hillslopes and increase of landslide occurrence (Edeso et al., 1999; Dhakal and Sidle, 2003).

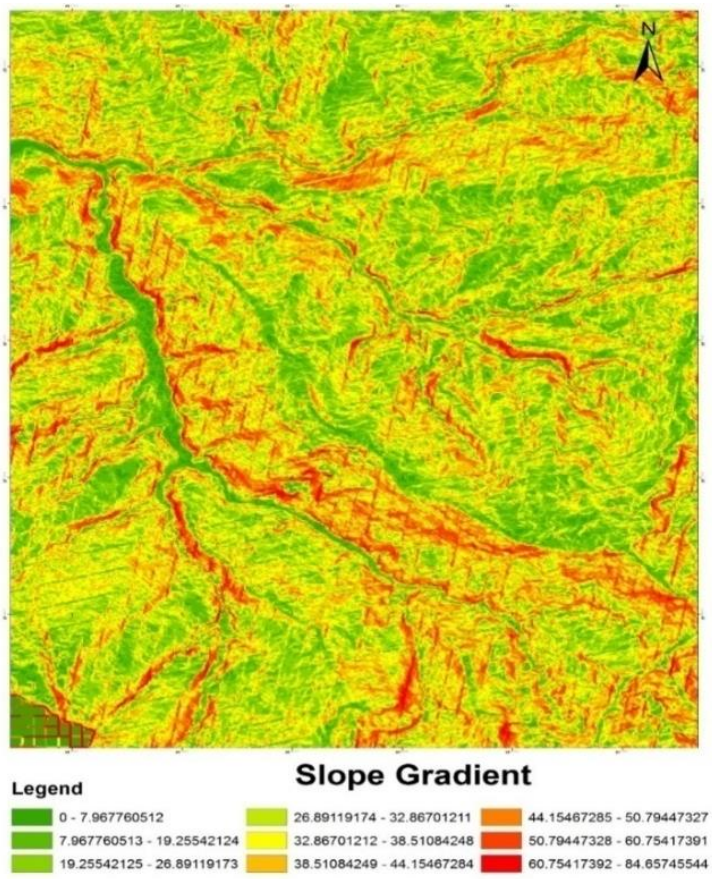

Figure 19. Slope map of the study area.

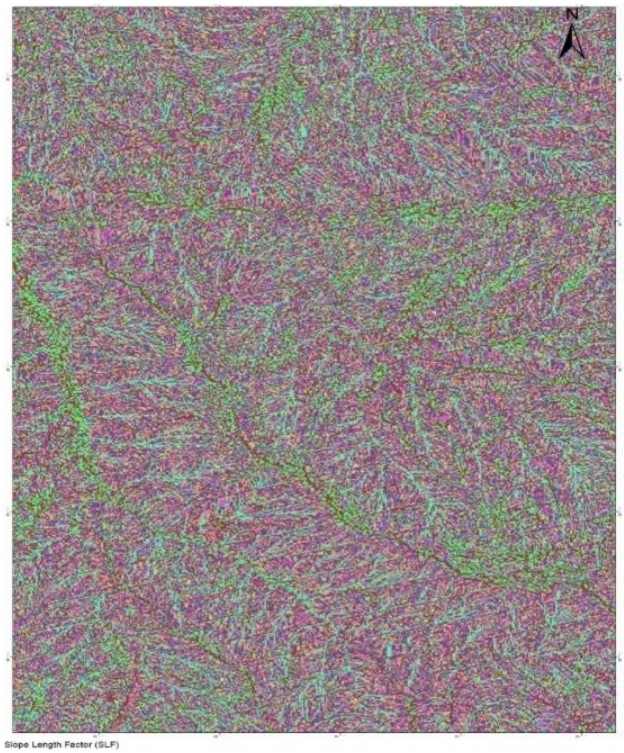

Figure 20. Slope length factor of the area.

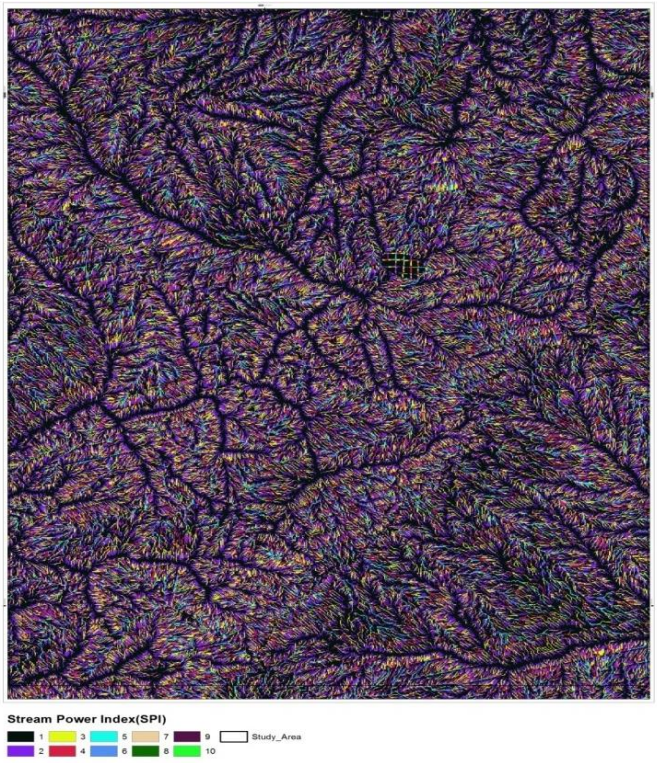

Figure 21. Stream power index of the area.

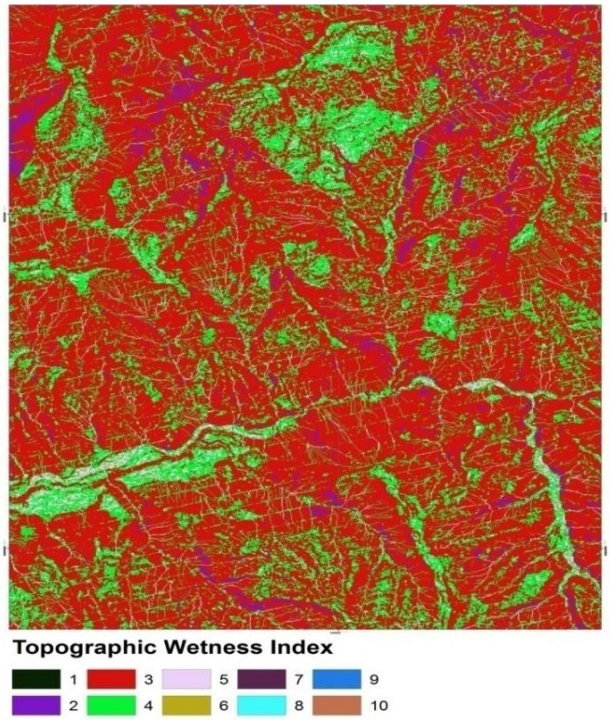

Figure 22. Topographic wetness index (TWI of the study area).

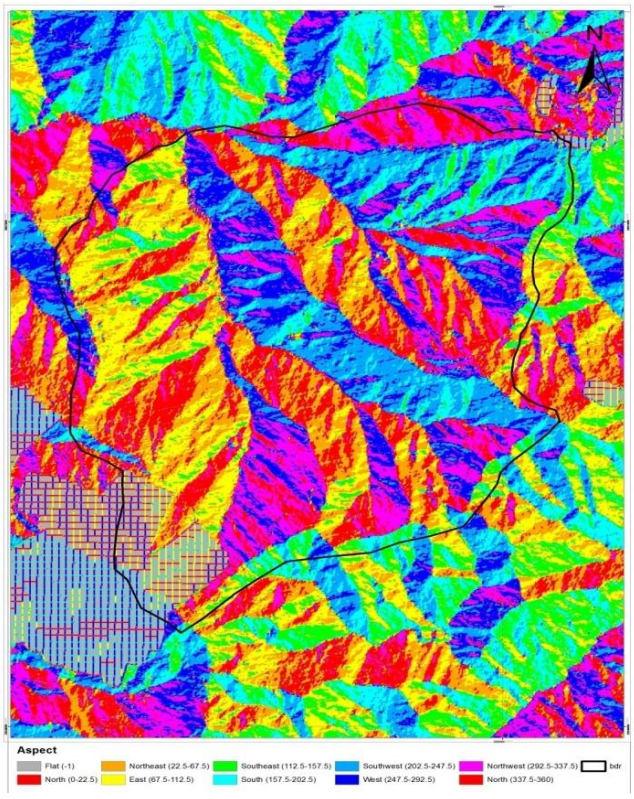

Figure 23. Aspect of the study area.

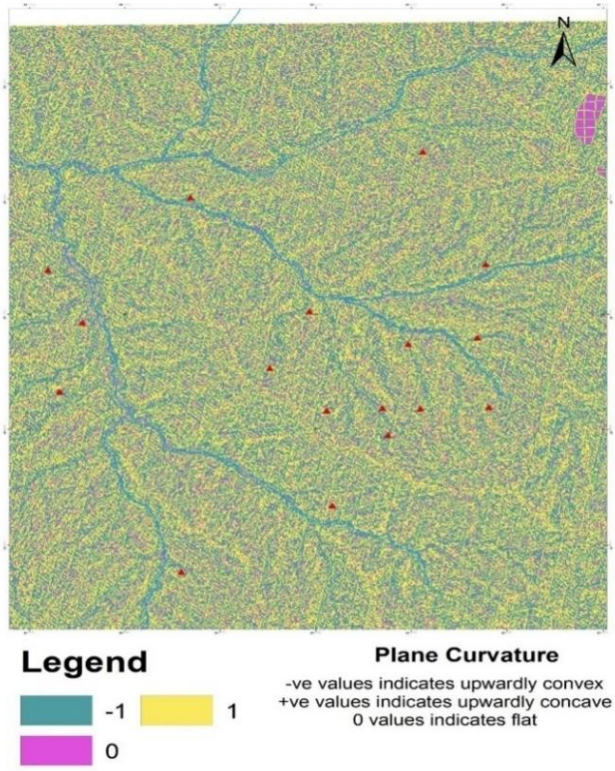

Figure 24. Plane curvature of the study area.

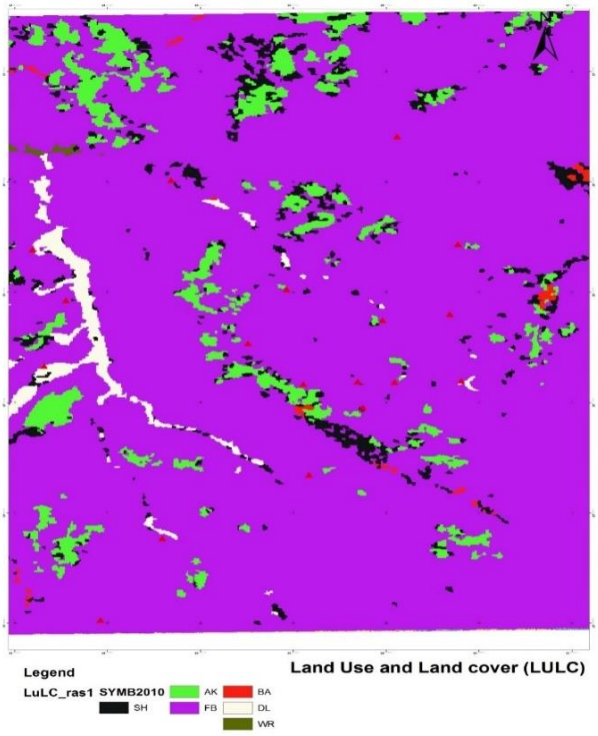

Figure 25. Land use and land cover map of the study area.

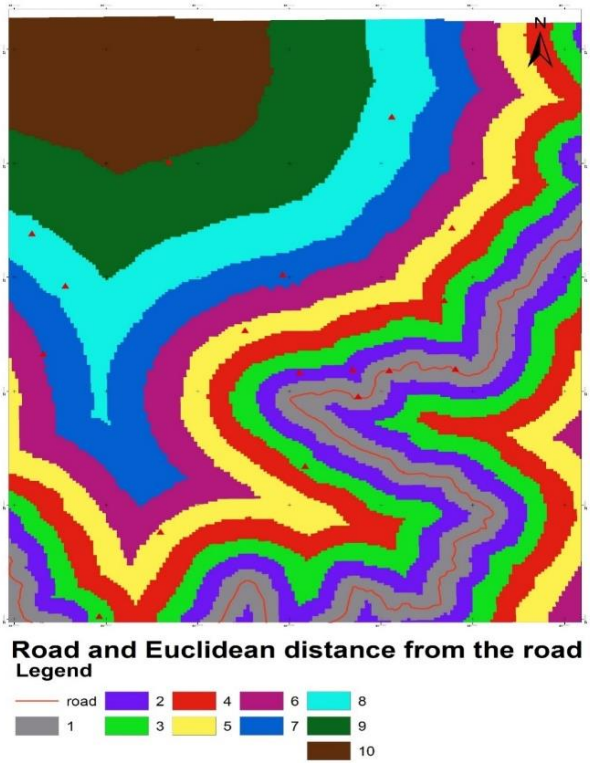

Figure 26. Distance from the road of the study area.

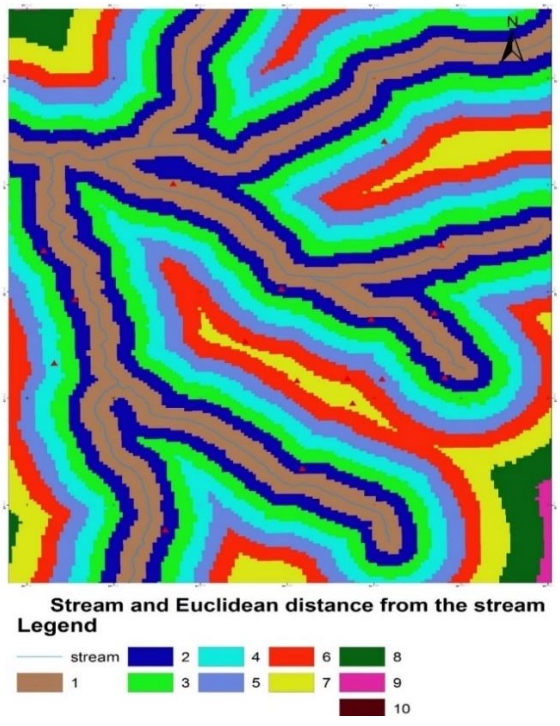

Figure 27. Distance from the stream of the study area.

4. APPLICATION OF MODELS IN LANDSLIDE HAZARD MAPPING

The general progression of landslide susceptibility mapping is illustrated in Figure 28. Landslide locations were identified using Google imageries and then verified with field survey. The landslides were then randomly divided into training (50% of landslide locations) and validation data (the remaining 50%). Topography, soil, forest, geology, and land-use datasets were also compiled in a spatial database, and the 8 landslide related factors were then extracted from the spatial database. Using probabilistic and statistic models, the relationships between landslide locations and each factor were calculated quantitatively and landslide-susceptibility maps were created based on these relationships. Based on those relationships, landslide susceptibility maps were then created. The landslide susceptibility maps were validated using the landslide locations that were not included in the training. The individual methods were compared according to their prediction accuracy. In this case studies, frequency ratio, weight of evidence and logistic regression models were applied to analysis landslide susceptibility. In the case of frequency ratio model is a brief overview of Park and Lee (2014)'s research as an application of frequency ratio model to analysis landslide susceptibility mapping.

4.1. FREQUENCY RATIO

The frequency ratio is a simple technique for producing a landslide susceptibility map, and it is highly compatible with GIS technology. The frequency ratio is the ratio between the area in which the landslide occurred and the class or type of a given factor in the case study area. To calculate the frequency ratio model for the class or type of each factor, all scale factors that consisted of a raster type were reclassified using GIS techniques into 10 classes based on equal areas. The cross tabulation in ArcGIS 10.2 was used to calculate the number of landslide occurrences in the class or type of each factor. The frequency ratio was used to calculate the ratio of the cell with landslide occurrence in each class for a reclassified factor or categorical factor (i.e., geology and land use), and the ratio was assigned to each factor class again. Finally,

the landslide susceptibility by frequency ratio was created using overlay functions in GIS, which are used to merge different factors assigned to the ratio.

The frequency ratio is the ratio of the area where landslides occurred to the total area, so a value of 1 means an average value. If the value is greater than 1, there is a high correlation, and if it's lower than 1, then there is a lower correlation. If the probability is high, there is a greater susceptibility for landslides; a lower value indicates a lesser susceptibility.

Using the frequency ratio model, the frequency ratio of each factor in each class range was calculated (Table 2 to Table 10). From the frequency ratio, the relationships between landslides and the examined factors were calculated as follows: the ratio for slopes of 38-70° was greater than 2, indicating a higher probability of landslides, and slopes from 0° to 26.2° was less than 1.0, indicating a lower probability. Landslides were found to be most abundant on the southwest-facing hill slopes, indicating that this aspect is highly susceptible. In the case of distance from the fault, the ratio was greater than 1 from 20.94 to 52.74 m, but less than 1 over 52.75 m. The ratio for TWI values from 3.60 to 4.89 was greater than 2, indicating a very higher probability of a landslide. Plan curvature values represent the morphology of topography. Positive curvature indicates that the surface is upwardly convex at that cell. Negative curvature indicates that the surface is upwardly concave. A zero value indicates that the surface is planar. The more negative or positive the value is, the higher the probability of landslide occurrence. Planar areas had a low value of 0.08. Plan curvature is thus related to landslides because runoff or retention of water after heavy rainfall occurs on more upwardly concave or convex slopes, respectively. Regarding land use, areas with traffic facilities such as roads, railroads, and reservoirs had a ratio of 1.48, indicating a high probability of landslides.

Using the probability model, the spatial relationship between the landslide occurrence location and each related factor was derived. The rating of each factor types or range was assigned as

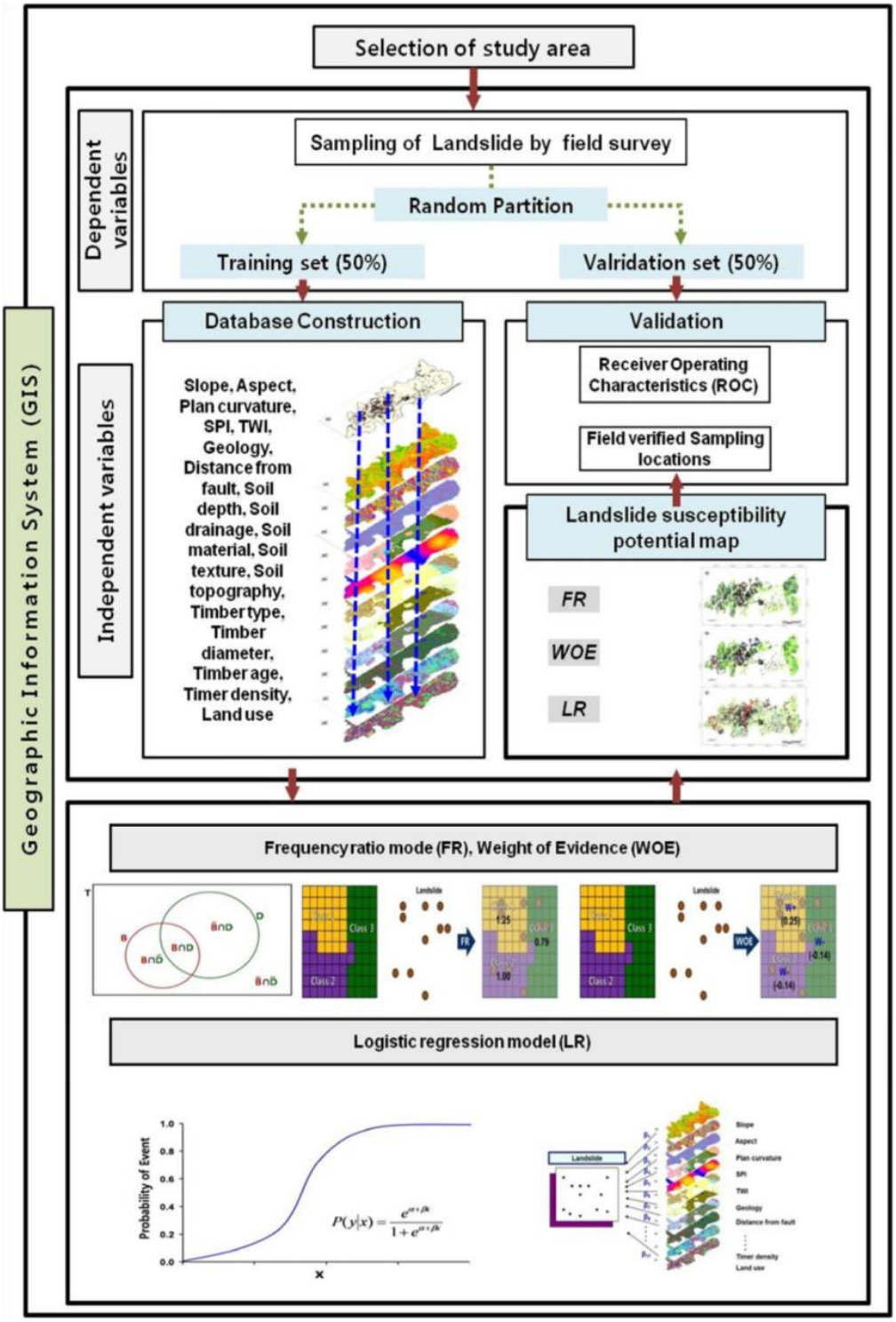

Figure 28. Work process flow chart of the study area.

the relationship between landslide location and each factor, which was the ratio of landslide-free to event-evident cells as shown in the Tables 2 to 10.

The landslide susceptibility index (LSI_{FR}), is calculated by a summation of each factor ratio value (Lee and Min, 2001) as shown below:

$$LSI_{FR} = FR_1 + FR_2 + FR_3 + \ldots\ldots\ldots\ldots\ldots\ldots\ldots\ldots\ldots\ldots + FR_n$$

Where, FR_n is a frequency ratio of each factor type or range.

To obtain a landslide-susceptibility map, the LSI values were reclassified into different susceptibility classes. Five classes were established based on the area for easy and visual interpretation: very high (10%), high (10%), medium (20%), low (20%), and very low (40%). Landslide susceptibility maps were created using the LSI and are shown in Plate IV.

The relationship between the landslide and related factor using frequency ratio model (Park and Lee, 2014) are provided (Tables 14 to 22).

Table 14. The relationship between landslide and slope.

Factors	class	Domain(D)	Domain%	Landslide(L)	landslide%	FR
Slope (Degree)	1	66377	9.65	0	0.00	0.00
	2	67535	9.82	100	2.22	0.23
	3	72069	10.48	300	6.67	0.64
	4	67765	9.85	600	13.33	1.35
	5	69360	10.08	200	4.44	0.44
	6	71077	10.33	600	13.33	1.29
	7	69183	10.06	900	20.00	1.99
	8	72138	10.49	500	11.11	1.06
	9	66158	9.62	900	20.00	2.08
	10	66195	9.62	400	8.89	0.92

Table 15. The relationship between landslide and SPI.

Stream Power Index (SPI)	Class	D	D%	L	L%	FR
	1	162235	28.60	1300	28.89	1.01000
	2	45222	7.97	0	0.00	0.00000
	3	45133	7.96	200	4.44	0.55855
	4	45169	7.96	300	6.67	0.83715
	5	45094	7.95	300	6.67	0.83854
	6	44979	7.93	200	4.44	0.56046
	7	45025	7.94	600	13.33	1.67966
	8	44691	7.88	400	8.89	1.12814
	9	44841	7.91	400	8.89	1.12437
	10	44811	7.90	800	17.78	2.25024

Table 16. The relationship between landslide and SLF.

Factor	Class	D	D%	L	L%	FR
Slope Length Factor (SLF)	1	162235	28.60	1300	28.88889	1.01
	2	45133	7.96	0	0	0.00
	3	45136	7.96	100	2.222222	0.28
	4	44974	7.93	300	6.666667	0.84
	5	44994	7.93	300	6.666667	0.84
	6	45037	7.94	300	6.666667	0.84
	7	45068	7.95	100	2.222222	0.28
	8	44889	7.91	900	20	2.53
	9	44759	7.89	400	8.888889	1.13
	10	44975	7.93	800	17.77778	2.24

Table 17. The relationship between landslide and TWI.

Factor	Class	D	D%	L	L%	FR
Topographic Wetness Index (TWI)	1	54925	10.01	400	8.89	0.89
	2	55282	10.07	1000	22.22	2.21
	3	54975	10.02	500	11.11	1.11
	4	55258	10.07	200	4.44	0.44
	5	55162	10.05	300	6.67	0.66
	6	54920	10.01	600	13.33	1.33
	7	54735	9.97	700	15.56	1.56
	8	54768	9.98	0	0.00	0.00
	9	54402	9.91	300	6.67	0.67
	10	54491	9.93	500	11.11	1.12

Table 18. The relationship between landslide and distance from road.

Factor	Class	D	D%	L	L%	FR
Road (Euclidean distance from road)	1	52878	10.32	500	11.11	1.08
	2	50697	9.90	600	13.33	1.35
	3	51206	10.00	900	20.00	2.00
	4	51546	10.06	300	6.67	0.66
	5	50719	9.90	800	17.78	1.80
	6	51196	10.00	300	6.67	0.67
	7	50951	9.95	300	6.67	0.67
	8	51136	9.98	500	11.11	1.11
	9	50977	9.95	100	2.22	0.22
	10	50867	9.93	200	4.44	0.45

Table 19. The relationship between landslide and distance from the stream.

Factor	D	D	D%	L	L%	FR
Stream (Euclidean distance from the river or stream)	1	69028	10.59	800	17.78	1.68
	2	66538	10.20	1200	26.67	2.61
	3	66170	10.15	200	4.44	0.44
	4	65019	9.97	400	8.89	0.89
	5	64100	9.83	500	11.11	1.13
	6	64702	9.92	500	11.11	1.12
	7	64846	9.94	700	15.56	1.56
	8	63776	9.78	100	2.22	0.23
	9	63998	9.81	100	2.22	0.23
	10	63904	9.80	0	0.00	0.00

Table 20. The relationship between landslide and LULC.

Factor	Class	D	D%	L	L%	FR
Land Use Land Cover	1	21776	4.04	100	2.22	0.55
	2	30704	5.70	0	0.00	0.00
	3	476631	88.46	4100	91.11	1.03
	4	1752	0.33	0	0.00	0.00
	5	6751	1.25	300	6.67	5.32
	6	1226	0.23	0	0.00	0.00

Table 21. The relationship between landslide and curvature.

Factor	class	D	D%	L	L%	FR
Curvature	-1	236686	44.11	2200	48.89	1.11
	0	61266	11.42	600	13.33	1.17
	1	238688	44.48	1700	37.78	0.85

Table 22. The relationship between landslide and aspect.

factor	Class	D	D%	L	L%	FR
Aspect	1	15054	2.81	0	0.00	0.00
	2	85415	15.92	800	17.78	1.12
	3	75135	14.00	1000	22.22	1.59
	4	60099	11.20	700	15.56	1.39
	5	43344	8.08	200	4.44	0.55
	6	52772	9.83	400	8.89	0.90
	7	65869	12.27	600	13.33	1.09
	8	69159	12.89	400	8.89	0.69
	9	69793	13.01	400	8.89	0.68

D: Number of pixels of each class
D (%): Domain/total pixels in the case study area
L: Number of pixels of landslide occurrences in each Domain
L (%): Landslide/total pixels of landslide occurrences in the case study area

4.2. LOGISTIC REGRESSION

Logistic multiple regression allows for the formation of a multivariate regression relationship between a dependent variable and several independent variables. The advantage over simple multiple regressions is the addition of an appropriate link function to the usual linear regression model. The variables may be continuous, categorical or any combination thereof. When the dependent variable has only two groups, logistic multiple regressions may be preferred over discriminate analysis because categorical data may also be used for several reasons (O'Hair and Reid, 1998).

In the present situation, the dependent variable is binary to represent the presence or absence of landslides. Quantitatively, the relationship between the occurrence and its dependency on several variables can be expressed as:

$$p = 1/ (1+ e^z)$$

where, p is the probability of an event occurring. In the present situation, p is the estimated probability of a landslide based only on the intrinsic properties, which we term *susceptibility*. The probability varies from 0 to 1 on an S-shaped curve, and z is the linear combination. It follows that logistic regression involves fitting the data to an equation of the form

$$z = b_0 + b_1x_1 + b_2x_2 + \ldots + b_nx_n$$

where b_0 is the intercept of the model, b_i (i = 0, 1, 2, …, n) are the slope coefficients of the logistic multiple regression model, and x_i (i = 0, 1, 2, …, n) are the independent variables (Dai and Lee, 2002).

The spatial databases of each variable were converted to ASCII files using ArcGIS in the statistical package SPSS 20. Using this approach, logistic multiple regression coefficients (B), the standard errors of slope coefficients (S.E), the Wals tests (Wals), the significance levels (Sig.), and the exponentiated slope coefficients (Exp(B)) of the related variables were calculated (Table 23). The coefficients were estimated using the maximum-likelihood model. Because the relationship between the independent variables and the probability was nonlinear in the logistic multiple regression model, an iterative algorithm was necessary to estimate the params (Oh et al., 2009). The output that corresponds to the Hosmer and Lemeshow Goodness-of-Fit test (Hosmer and Lemeshow, 2000) was less than 0.05, which signified a good fit of the logistic regression model. After interpretation, an equation to predict the probability of landslide occurrence was created:

Z=(-0.007xSLOPE) + (-0.005xCURVATURE) + (-0.006xTWI) + (-0.025xSPI) + (0.20xDISTANCE FROM STREAM) + ASPECT+GEOLOGY + LANDUSE-51.631.

Here, SLOPE is the slope value, CURVATURE is the curvature value, SPI is the spi value, TWI is the twi value, and DISTANCE FROM STREAM AND ROAD is the distance from

the stream and road value. ASPECT, GEOLOGY, LAND USE, SLOPE and Z is a prediction param.

Using the logistic regression coefficient (Table 23) and two equations provided above, the probability of a species was computed and mapped as the landslide susceptibility index (LSI).

The latter was calculated using the logistic regression model for the interpretation. The index consisted of five classes based on the area for easy visual interpretation. Index ranges of very high, high, moderate, low, and very low in 5%, 10%, 15%, 20%, and 50% of the case study area, respectively, were used. The classification was useful to visually delineate the predicted landslide-susceptible areas.

5. VALIDATION

A landslide hazard or susceptibility map should effectively predict future landslide susceptibility areas and can be validated by incorporating data from new landslide locations as they occur. Here, the result of the landslide susceptibility analysis was validated using test landslide-area data (50% of total landslide area) that had not been used for the analysis. To validate the landslide susceptibility map, the calculated landslide susceptibility index values of all cells were sorted in descending order. The ordered cell values were then divided into 100 classes with accumulated 1% intervals. The above procedure was also adapted for cells in which a landslide occurred by comparing the 100 classes obtained with the distribution on the case study area. A graph was then generated by connecting the two classified values.

For example, in the case of the decision tree model, the 90-100% (10%) class of the case study area where the landslide susceptibility index rank was higher could explain 51% of the entire landslide. In addition, the 80-100% (20%) class of the case study area where the landslide susceptibility index rank was higher could explain 68% of the landslide. To quantitatively compare the results, the areas under the curve (AUC) were

re-calculated as the total area (Lee and Dan, 2005; Lee and Sambath, 2006). Thus, the area under a curve can be used to qualitatively assess the prediction accuracy.

Probabilistic (frequency ratio and weight of evidence) and statistics (logistic regression) approaches produced AUC values (Figure 29) from the validation of the landslide susceptibility maps, meaning that the landslide susceptibility maps had accuracies of 80.15% (frequency ratio), 74.73% (weight of evidence), and 75.92% (logistic regression).

Table 23. The output of logistic regression analysis.

Factor		B	S.E	Wals	Sig.	Exp(B)
Slope gradient (˚)		-0.007	0.000	273.401	0.000	0.993
Curvature		-0.005	0.002	4.284	0.038	0.995
TWI		-0.006	0.008	0.663	0.416	0.994
SPI		0.020	0.003	57.420	0.000	1.020
Distance from Stream		-0.025	0.017	2.054	0.152	0.976
Aspect	No Data	-0.229	0.033	717.704	0.000	0.796
	Residential Area	0.156	0.028			1.169
	Manufacturing Area	-0.440	0.086			0.644
	Commercial Area	0.489	0.032			1.630
	Recreational Area	-0.116	0.095			0.891
	Trafficked Area	0.180	0.031			1.197
	Public Area	0.000	0.000			0.000
Geology	Non-Green Farm	-0.079	0.050	517.979	0.000	0.924
	Paddy	-1.814	0.106			0.163
	Field	-1.171	0.084			0.310
	Orchard	-16.906	1901.109			0.000
	Other Plantations	-17.699	2883.907			0.000
	Natural Grassland	-0.525	0.385			0.592
	Grassland	-0.252	0.068			0.777
	Barren Ground	0.000	0.000			0.000
Lands use	No Data	1.485	0.335	19.647	0.000	4.414
	Retarding basin	0.000	0.000			0.000
Topography	No Data	1.485	0.335	19.647	0.000	4.414
	Retarding basin	0.000	0.000			0.000

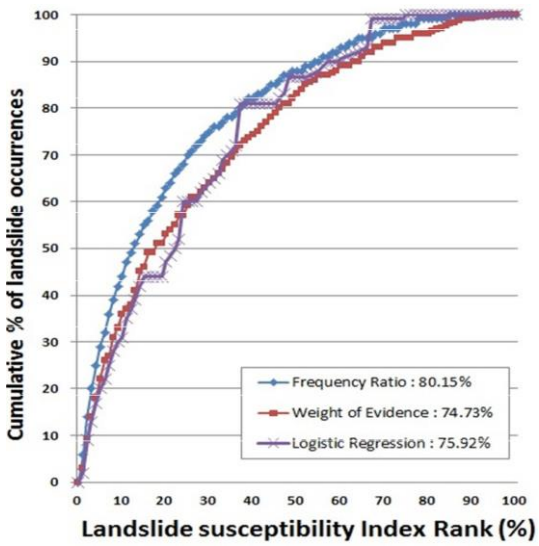

Figure 29. Cumulative frequency diagram showing landslide susceptibility, index rank occurring in the cumulative percentage of the landslide locations.

6. RISK ANALYSIS

The risk analysis for Moshiland slides has been performed to understand the overall risk scenario of landslides in the region. The risk is a product of vulnerability and hazard. Hence, the results from hazard mapping are crucial for risk analysis. As a part of vulnerability analysis, detail socio-economic data were collected. These data were overlaid on the hazard map to analyze the landslide related risk in the region (Plate IV). Two major risks are identified in the area: (1) the Samdrupjongkhar-Trashigang national highway is directly exposed to the landslide hazard. The highway passes right across the two Moshi landslides (Landslide-1 and Landslide 2). This highway is very important for people of Trashigang dzongkhag. The highway serves as the only means of communication between Trashigang and Samdrupjongkhar. The highway is often blocked by these landslides. About 300 m of this highway is within the landslide area. Hence, proper planning and implementation of mitigation or remedial measures are necessary to reduce risks to commuters and economy. These landslides also pose high-risk to the nearby human settlement, where several houses are located nearby or within the landslides and high-risk zone.

7. DISCUSSION, CONCLUSIONS AND RECOMMENDATIONS

This study used probabilistic (frequency ratio) and Statistical (logistic regression) models to predict areas susceptible to landslides in the Moshi-Tshogoenpa-Lumang watershed and surrounding areas, where landslides are expected to continue in the future. The frequency-ratio model indicated landslide susceptibility on steep slopes, southwest-facing hillslopes, and slopes which are 20.94 to 52.74 m from the stream. Moreover, landslides tend to occur in areas of highly negative or positive plan curvature, areas of high traffic, mountainous areas, and the colluvium deposits areas.

Probabilistic (frequency ratio and logistic regression) approaches produced AUC values from the validation of the landslide susceptibility maps. The result maps from other models also exceeded 70%: 80.15% (frequency ratio), and 75.03% (logistic regression). This study identified factors that are being involved in landslides and the results and hence the method is used to map the landslide susceptibility in the region. Landslide hazard or susceptibility map can be used to prepare risk map to aid in mitigating risk to people and facilities and serve as basic data for plans to prevent landslide hazards, such as in locating monitoring and facility sites.

The social elements such as human settlements and highway that are located nearby or within high-hazard zone needs immediate attention in terms of scientific-based planning and implementation of mitigation measures to reduce risks. The medium hazard areas where social elements are located within or nearby it is recommended for detailed geological studies to assess the hazard and risk in detail and make scientific-based recommendations on implementation of mitigation measures to reduce risks.

7. ACKNOWLEDGEMENT

The authors are very grateful to Mr Phuntsho Tobgay, Director General; Mr Ugyen Wangda, Chief Geologist of Geological Survey Division; and Mr Tashi Tenzin, Project Manager of DGM for their leadership, support, guidance and feedback provided during fieldwork and report and map preparation. The support and guidance rendered by

NAPA-II Project Manager Ms Sonam Lhaden Khandu; current Project Support Officer Mr Netra Sharma and all previous Project Support Officers; Mr Ugyen Dorji; NAPA-II focal person from UNDP; current and past Project Directors from NEC; Board Chair and Members; and all other people who were directly or indirectly involved in this project are well appreciated. Our gratitude also goes to Mr. Netra Sharma for improving this report by proof-reading the final draft and providing valuable comments. We also thank all government agencies, NGOs, and people who have provided help during fieldwork and feedback during the National Workshop held on this project at Phuentsholing from 13-14 November 2017. Lastly, on behalf of DGM, we sincerely extend our gratitude to LDCF-GEF and UNDP for providing funding and technical support, without which, this study would not have been achieved.

8. REFERENCES

Adinarayana, J., Krishna, N. R., 1996, Integration of multi-seasonal remotely sensed imageries for improved land use classification of a hilly watershed using geographical information systems: International Journal of Remote Sensing 17, 1679-1688.

Aggett, G. R., Wilson, J. P., 2009, Creating and coupling a high-resolution DTM with a 1-D hydraulic model in a GIS for scenario-based assessment of avulsion hazard in a gravel-bed river: Geomorphology, v. 113, p. 21-34.

Agterberg, F. P., 1988, Application of recent developments of regression analysis in regional mineral resource evaluation: Quantitative Analysis of Mineral and Energy Resources, v. 223, p. 1-28.

Bhargava, O. N., 1995, The Bhutan Himalaya: a Geological Account. Geological Survey of India Special Publication, v. 39, 245 p.

Coduto, D. P., Yeung, M. R., and Kitch, W. A., eds, 2011, Geotechnical Engineering: Principles and Practices: Pearson, 814 p.

Cruden, D. M., Varnes, D. J., 1996, Landslide Types and Processes, Special Report, Transportation Research Board, National Academy of Sciences, v. 247, p. 36-75.

Hungr, O., Corominas, J., Eberhardt, E., 2005, Estimating landslide motion mechanism, travel distance and velocity. In: Hungr O, Fell R, Couture R, Eberhardt E (eds) Landslide Risk Management, Taylor & Francis, London, p. 99-128

Hungr, O., Evans, S. G., 1996, Rock avalanche runout prediction using a dynamic model, In: Senneset K (ed) International Symposium on Landslides, Trondheim, p. 233-238

Hungr, O., Evans, S. G., 2004, Entrainment of debris in rock avalanches: An analysis of a long run-out mechanism. Geological Society of America Bulletin, v. 116, p. 9-10.

Lee, S., and MIN, K., 2001, Statistical analysis of landslide susceptibility at Yongin, Korea Environmental Geology, v. 40, p. 1095–1113.

LEE, S., CHOI, J. and MIN, K., 2004a, Probabilistic landslide hazard mapping using GIS and remote sensing data at Boun, Korea: International Journal of Remote Sensing, v. 25, p. 2037–2052.

Long, S., McQuarrie, N., Tobgay, T., Grujic, D., and Hollister, L., 2011c, Geologic map of Bhutan. Journal of Maps, v. 7, p. 184-192.

Susumo Sato, JoVC, 2003, Survey manual (Unpublished).

Thapa, T. P., 2013, Report on Technical Feasibility Study for the Four Critical Landslides within the Extended Township of Phuentsholing: Geological Survey of Bhutan, DGM, Thimphu.

Report printed at Kuensel Corporation Ltd., Thimphu: Bhutan

Engineering Geological & Proposed Remedial Measure Map of Moshi Slide No.1

Lumang Gewog, Wamrong Dungkhag, Trashigang Dzongkhag,

Scale: 1:1,000

Contour Interval : 2m

Season: February-June, 2015

NORTH

Moshi

Wamrong

A

A'

Legend

Remedial Measure Index

- Benching
- Wall
- Garland/Catch water drain
- French Drain

Geological/Topographical Legend

- Bedding
- Quartzite Outcrop
- Phyllite Outcrop
- Electric Pole
- Seepage
- Stream
- Tension Crack
- Sheer zone
- Cross-section
- Landslide Boundary/Crown
- Contour
- Road
- Building/House
- Cultivation Land
- Colluvium
- Phyllite
- Quartzite with Phyllitic parting

Geology by:	Surveyed by:
1. T.P Thapa (Executive Geologist)	1. Kinzang Duba (Survey Engineer)
2. Jamyang Chophel (Sr. Geologist)	2. Jampel Gyeltshen (Survey Engineer)
3. Nidup Wangmo (Geologist)	3. Hem Pradhan (Surveyor)

Engineering Geological & Proposed Remedial Measure Map of Moshi Slide No.2

Lumang Gewog, Wamrong Dungkhag, Trashigang Dzongkhag.

Scale: 1:1,000

Contour Interval : 2m

Season: February-June, 2015

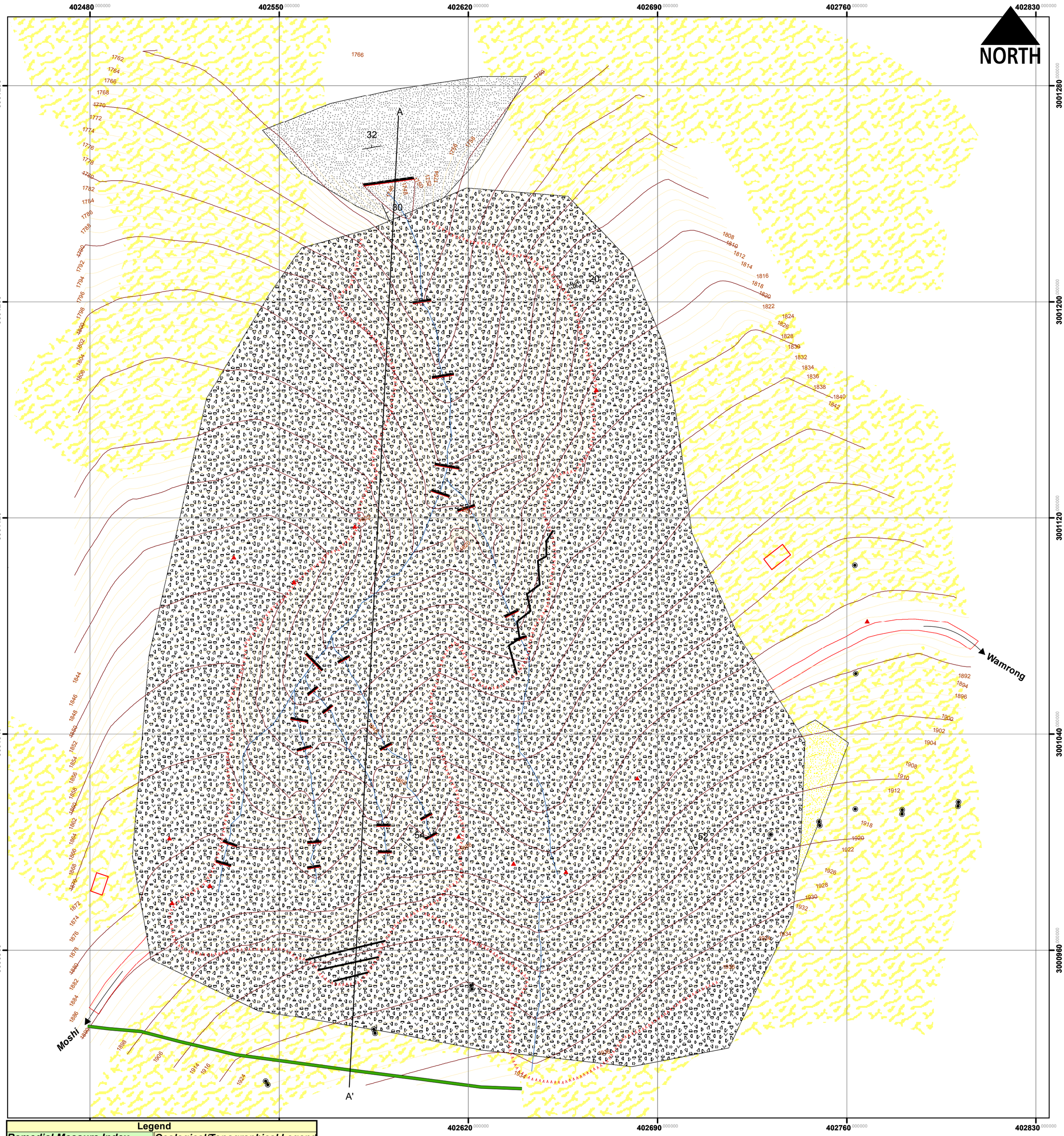

Legend

Remedial Measure Index

- Benching
- Wall
- Garland/Catch water drain
- French Drain
- Gabion Wall

Geological/Topographical Legend

- Bedding
- Electric Pole
- Stream
- Landslide Boundary/Crown
- Contour
- Road
- Building/House
- Cultivation Land
- Cross-section
- Colluvium
- Phyllite
- Quartzite with phyllite parting

Geology by:

1. T.P Thapa (Executive Geologist)
2. Jamyang Chophel (Sr. Geologist)
3. Nidup Wangmo (Geologist)

Surveyed by:

1. Kinzang Duba (Survey Engineer)
2. Jampel Gyeltshen (Survey Engineer)
3. Hem Pradhan (Surveyor)

Engineering Geological and Proposed Remedial Measure Map of Moshi Slide No.3

Wamrong Dungkhag, Lumang Gewog, Trashigang Dzongkhag.

Scale: 1:1,000

Contour Interval : 2m

Season: February-June, 2015

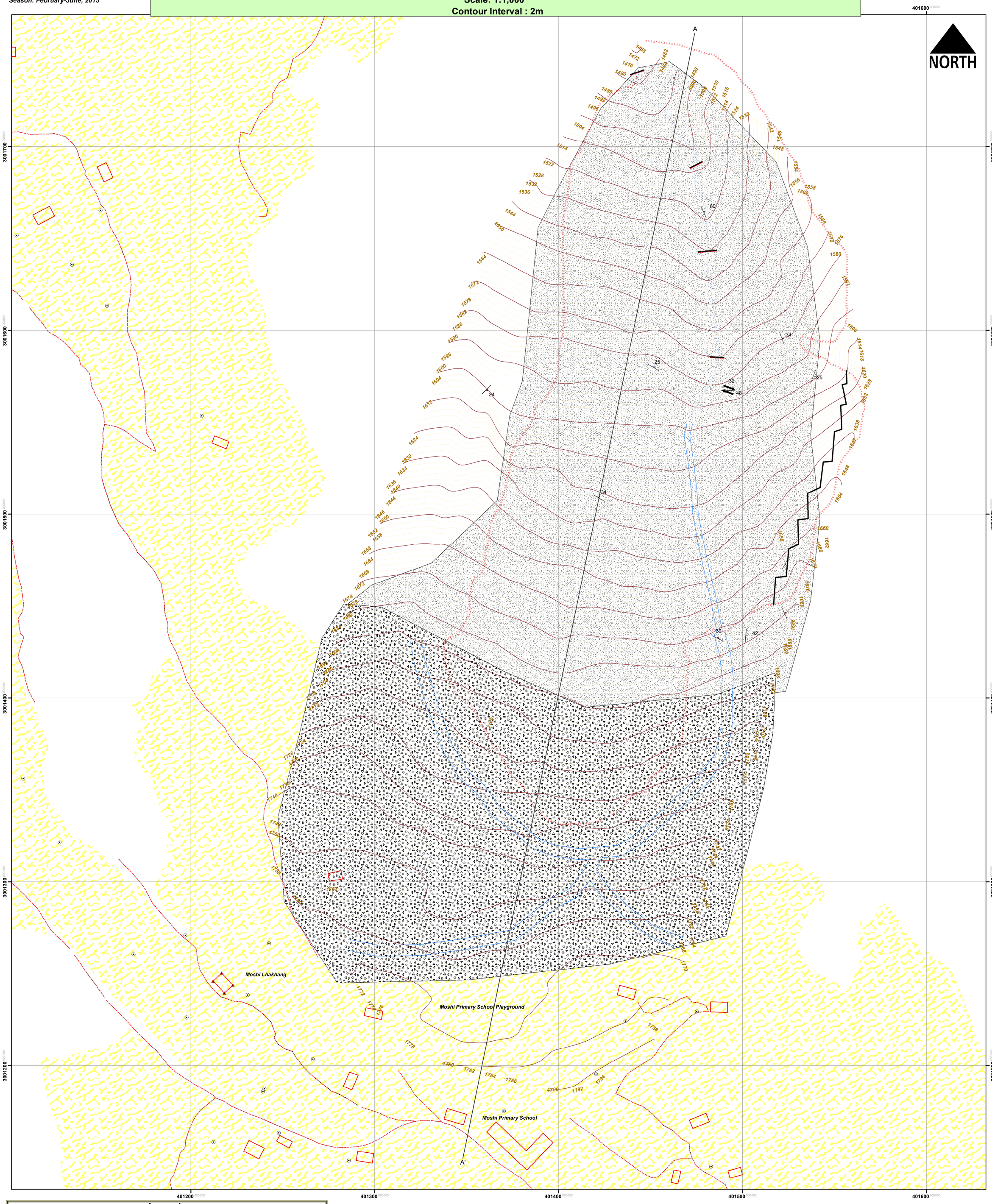

Legend

Remedial Measure Index	Geological/Topographical Legend
Benching	Bedding
Retaining Wall	Electric Pole
Garland/Catch water drain	Stream
French Drain	Landslide Boundary/Crown
Gabion Wall	Contour
	Road
	Building/House
	Cultivation Land

- Cross-section
- Colluvium
- Phyllite with occassional parting of quertzite

Geology by:

1. T.P Thapa (Executive Geologist)
2. Jamyang Chophel (Sr. Geologist)
3. Nidup Wangmo (Geologist)

Surveyed by:

1. Kinzang Duba (Survey Engineer)
2. Jampel Gyeltshen (Survey Engineer)
3. Hem Pradhan (Surveyor)

The Landslide Hazard Map of the Moshi-Tshogoenpa-Lumang Watershed

Scale 1:5000

Season 2014-15

N

353000 354000 355000 356000

3002000 3001000 3000000 2999000

Riserboo

Moshi

Ishogoenpa

Datum: WGS84 Projection: UTM

Prepared By: Jampel Gyeltshen, Survey Engineer

Legend

- social Infrustucture
- Stream
- Highway

Landslide Hazard

- Low Hazard
- Medium Hazard
- High Hazard